European Commission

JRC TECHNICAL REPORTS

Analysis of the water-power nexus in the West African Power Pool

Water-Energy-Food-Ecosystems project

DE FELICE, M.,
GONZÁLEZ APARICIO, I.,
HULD, T., BUSCH, S.,
HIDALGO GONZÁLEZ, I.

2019

EUR 29617 EN

Contact information
Name: Matteo De Felice
Address: European Commission, Joint Research Centre, P.O. Box 2, NL-1755 ZG Petten, The Netherlands
Email: Matteo.DE-FELICE@ec.europa.eu
Tel.: +31 22456-5160

EU Science Hub
https://ec.europa.eu/jrc

JRC115157

EUR 29617 EN

PDF ISBN 978-92-79-98138-8 ISSN 1831-9424 doi:10.2760/362802

Luxembourg: Publications Office of the Eur opean Union, 2019

How to cite this report:
DE FELICE, M., GONZÁLEZ APARICIO, I., HULD, T., BUSCH, S., HIDALGO GONZÁLEZ, I., *Analysis of the water-power nexus in the West African Power Pool - Water-Energy-Food-Ecosystems project*, EUR 29617 EN, Publications Office of the European Union, Luxembourg, 2019, ISBN 978-92-79-98138-8, doi:10.2760/362802, JRC115157.

Contents

Acknowledgements

We would like to thank the following colleagues for the contributions provided:

— related to the LISFLOOD model: Marko Adamovic, Berny Bisselink, Ad de Roo

— the Dispa-SET model and power system-related questions: Konstantinos Kavvadias, Konstantinos Kanellopoulos, Hrvoje Medarac

— the comments and insights on the hydrological inputs and assumptions: Ioannis Kougias, Cesar Carmona Moreno, Fabio Farinosi, Paolo Ronco.

Authors

Matteo De Felice

Iratxe González Aparicio

Thomas Huld

Sebastian Busch

Ignacio Hidalgo González

Abstract

The operation and economics of the power systems are constrained by the availability and temperature of water resources since thermal power plants need water for cooling and hydropower plants are fuelled by water to generate electricity. In Europe and North America water shortages or high river water temperatures have recurrently occurred in the last years, leading to financial losses, power curtailments, temporary shutdowns, demand restrictions, and ultimately increased wear and tear of the power plants. On the other hand, the operation of the power system may impact on the quantity and quality of the water resources.

The combined effect of increased water consumption, for energy and non-energy purposes, with lower availability of water resources due to climate change is expected to lead to similar problems in Africa. In most African energy systems hydropower is the dominant renewable energy source, but they rely heavily on oil- and gas-fired capacity, and lack interconnections with neighbouring countries.

This technical report describes the modelling framework developed by the JRC for analysing the water-power nexus, the input data and assumptions, the results of two scenarios for the West African Power Pool (WAPP), and conclusions derived from the analysis.

The results show that the proposed model behaves soundly, despite the data-related limitations, replicating the available statistics up to a great extent. Furthermore, the simulation was able to provide hourly time-series of electricity productions at plant-level in a robust way, since that the modelling is based on long time-series of climate data. We show that currently the operation of the WAPP power system significantly depends on the availability of water resources, not only for the use of hydro-power generation but also for the cooling of thermal power plants. This dependence translates into a high volatility of the system cost which would be reduced by the thermal capacities scheduled to be commissioned in the WAPP in the near-future. As a consequence, in the long term, the dependence of the power system on water resources could become even more important to meet the increasing electricity demand in the WAPP.

1 Introduction

The water-energy nexus is the term used to refer to the complex interactions between the water sector and the energy sector [1], [2]. On the one hand, water is needed for energy production, fossil-fuel extraction, transport and processing, or irrigation purposes. On the other hand, energy is needed for extraction, treatment, and distribution of drinking water, and for wastewater treatment and desalination [2]. One aspect of this conundrum is the link between water and electric energy (also known as water-power nexus or water-electricity nexus) when it comes to its quantification within the electric power system [3]–[5].

Within the electricity sector context, the operation and economics of the power systems are constrained by the availability and temperature of water resources since thermal power plants need water for cooling and hydropower plants are fuelled by water to generate electricity. Regarding the thermal power plants, the largest amount of freshwater withdrawals for cooling purposes can be found in North America and Europe representing 86% of the global water withdrawals [6], whereas the water used for cooling represents 43% of the European Union's water demand [6], [7]. Due to water shortages or high river water temperatures, 'the number of days with a reduced useable capacity is projected to increase in Europe and USA' according to the Fifth Assessment Report of the Intergovernmental Panel on Climate Change (IPCC) [8]. In fact, water impacts on European power systems have recurrently occurred in the last years and they led to monetary losses, power curtailments, temporary shutdowns, demand restrictions, and ultimately increased wear and tear of the power plants (see [9] and references therein). On the other hand, the operation of the power system may impact on the quantity and quality of the water resources.

The combined effect of increased water consumption, for energy and non-energy purposes, with lower availability of water resources due to climate change is expected to lead to similar problems in Africa. According to the World Bank[1], electricity and water demands are projected to grow significantly up to 2050 in Africa, by 700% and 500% respectively, with respect to 2012. In most African energy systems hydropower is the dominant renewable energy source. Other salient characteristics of these systems are their small sizes, the low electrification rates, the high shares of oil in the power generation mix, and the lack of significant power and gas interconnections.

The Joint Research Centre of the European Commission (JRC) has developed a fruitful cooperation with the African Union and its institutions, in line with the EU-Africa Strategic Partnership[2]. This cooperation aims to provide evidence-based scientific and technical support to decision makers, as well as to universities, research institutes and the scientific community at large, thus also contributing to the fulfilment of the objectives defined at the Rio+20 United Nations Conference on Sustainable Development[3]. Water and renewable energy feature among the key priority areas for cooperation.

This report describes the modelling framework developed by the JRC for analysing the water-power nexus, in the framework of the Water-Energy-Food-Ecosystems project (WEFE). WEFE is an internal JRC project that supports the design and implementation of cross-sectoral policies looking to improve the resilience of water-using sectors and the preservation and sustainability of freshwater resources.

The approach discussed in the next sections has been tested for the West African Power Pool[4] (WAPP). This area has been selected for several reasons[5]:

— The WAPP region[6] has a significant rate of economic growth, with demand for water, food and energy on the rise.

[1] World Bank's Thirsty Energy Initiative: http://www.worldbank.org/en/topic/water/brief/water-energy-nexus.
[2] See https://www.africa-eu-partnership.org/en and http://www.aeep-forum.org/en/home.
[3] https://sustainabledevelopment.un.org/rio20.
[4] http://www.ecowapp.org/.
[5] http://www.ecreee.org/sites/default/files/ecreee_policy_briefpolicy_brief_managing_resources_for_sustainable_devel.pdf

— The WAPP member states are also considered highly vulnerable to climate change and are already experiencing impacts on their agricultural productivity, food, water, and energy security.

— The area is rich in water resources (approximately 27% of Africa's internal renewable water resources), but suffers from chronic water deficits because of uneven distribution of rainfall and flows in time and space, insufficient knowledge about water resources, low allocation of potential resources, and poor resource management.

— The region has plenty of energy resources but they are also unevenly distributed, and the renewable energy potential is underused. Electrification rates are low and there is a high dependence on biomass. The power generation mix has a significant share of gas and oil power plants and the interconnections between countries are very limited.

— The goal of WAPP is to integrate the national power systems into a unified regional electricity market with the ultimate goal of providing in the medium and long term, a regular and reliable energy at competitive cost, under the auspices of the Economic Community of West African States[7]. For that purpose there exists an ongoing cooperation to promote and develop power generation and transmission infrastructures as well as to coordinate the exchange of power among the WAPP member states.

The overall objective of this report is to show that the proposed modelling framework may be used to analyse the water-power nexus in large areas, such as the WAPP, with a high temporal and spatial resolution and with the most accurate data. Specifically, this work aims to:

— Present the methodology for the analysis of the water-power nexus.

— Describe the available public data sources used for modelling the WAPP case study.

— Validate the proposed approach comparing the outcomes of the model with the available historical data and testing the behaviour of the model in a near-future scenario. This is accomplished by applying the framework presented in [10], which consists of combined use of the Dispa-SET [10], [11] and LISFLOOD [12] models. Then, the reservoir levels are passed on to the Dispa-SET Unit Commitment and Dispatch (Dispa-SET UCD) module [11], which runs for one year at hourly time steps.

This study also serves as a basis for possible future capacity building activities by providing a set of open source tools and data that can be used by researchers or practitioners across the region. In particular, this study is expected to:

— Serve as a proof of concept of a methodological approach for analysing scenarios with high penetration rates of electricity from renewable energy sources (RES-E) in African power systems. This methodology, based on open models and data, could be used by policy makers, regulators, transmission system operators and investors taking informed decisions.

— Produce a good estimation, using new methods applied to publicly available data, of key data currently missing needed for analysing the water-power nexus, in particular i) time series with hourly load profiles, ii) time series of wind and solar availability factors, and iii) gaps in power system infrastructure and reservoir datasets. All those data are the minimum inputs needed for addressing storage and flexibility needs in African power systems.

— Lay the foundations for carrying out studies on geographically and technologically optimised high RES-E systems for the African continent.

The document is divided in the following chapters:

---

[6] Consisting of Benin, Burkina Faso, Cape Verde, Ivory Coast, Gambia, Ghana, Guinea, Guinea Bissau, Liberia, Mali, Niger, Nigeria, Senegal, Sierra Leone and Togo. All the analysis has been made at national level, considering each country of WAPP as a node of the system (except Cape Verde which is disconnected from the rest of the system).

[7] http://www.ecowas.int/

— Chapter 2 describes the mathematical approach used to model the water-power nexus.

— Chapter 3 describes all the data and the assumptions used in the analysis.

— Chapter 4 explains the results of the two scenarios envisaged for the WAPP system, used to validate the methodology.

— Finally, chapter 5 contains the main conclusions of the study and describes further research planned in the framework of the WEFE project.

2 Model formulation

The modelling of the WAPP area is based on the power system model Dispa-SET [13] which consists of a mid-term hydrothermal coordination (MTHC) and a unit commitment and dispatching (UCD) module.

The proposed framework to address water-power nexus studies is presented in Figure 1. In this figure, we can see that both modules of Dispa-SET are linked to the rainfall-runoff hydrological LISFLOOD model [12] in an off-line mode. The steps are explained next:

— Step 1: LISFLOOD is solved to feed water inflows and water demands into the Dispa-SET model, which would impose constraints on hydropower plants and water-constrained limitations in thermal power plants.

— Step 2: Dispa-SET MTHC model runs at daily time steps during one or several years in order to simulate the management of water resources in the mid-term, i.e. the reservoir levels from the dams are passed on to shorter-term problems. As mentioned earlier, water values for hydropower sources are an outcome of this model.

— Step 3: Dispa-SET UCD model runs at hourly time steps during a target year and the following results can be obtained: 1) the power schedule and dispatch, 2) water-related outcomes (e.g. water withdrawn and consumed by power plants), and 3) economic results (prices and costs).

Note that ideally Dispa-SET MTHC and LISFLOOD should be run iteratively until reaching a stable solution. The stopping criteria may be based on the reservoir levels so that a set of adequate and optimised levels is derived. However, this issue should be further investigated and the methodology is non-iterative.

Figure 1. Diagram of the modelling chain

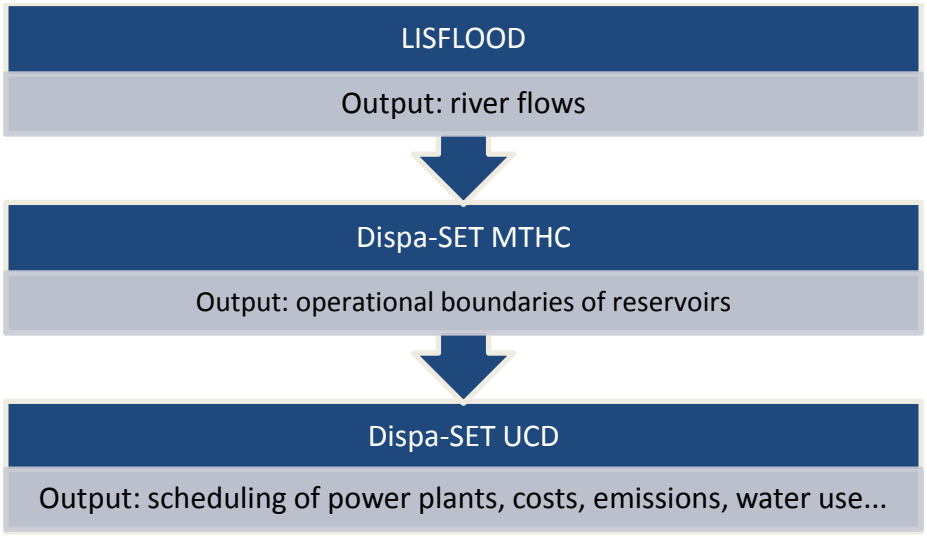

2.1 The Dispa-SET mid-term hydrothermal coordination module (Dispa-SET MTHC)

The aim of this module is to establish the operational limits of the reservoir levels of the hydro-power plants for each year of simulation. Those levels will be used in a later stage as boundaries by the unit commitment module.

This module is implemented as a constrained linear programming problem in GAMS [14].

Table 1. Model parameters

Name	**Unit**	**Description**
Demand(t,n)	GW	Electricity demand for the node *n* at time *t*
Pmin(u), Pmax(u)	GW	Minimum and maximum generation for the unit *u*
VarCost(u)	K€/GWh	Variable cost of generation for the unit *u*
StInit(u), Stmin(u), Stmax(u)	Hm^3	Initial, minimum and maximum amount of stored water
Delay(u_1, u_2)	days	Water transport delay between two reservoirs
NominalHead(u)	m	Nominal head of a dam
Inflow(t,u)	m^3/s	Natural inflow for the plant *u* at time *t*
Evaporation(t,u)	m^3/s	Evaporation for the plant *u* at time *t*
LineCapacity(l)	GW	Transmission line capacity
Demand_water(t,u)	m^3/s	Water withdrawal for the plant *u* at time *t*
$\eta(u)$	-	Efficiency of the turbine *u*
Ecological_flow(t,u)	m^3/s	Environmental flow for the unit *u*
Spillage_max(t,u)	m^3/s	Maximum spillage allowed for the unit *u*

Table 2. Model variables

Name	**Unit**	**Description**
G(t,u)	GWh	Energy generated at time *t* by the unit *u*
PUMP(t,u)	GWh	Energy pumped by the unit *u*
RES(t,u)	Hm^3	Water stored in reservoir associated to plant *u* at time *t*
DIS(t,u)	m^3/s	Water discharge by plant *u*
CH(t,u)	m^3/s	Water charged to pumped hydro storage for plant *u*
SPILL(t,u)	m^3/s	Spilled water at plant *u*
FLOW (t,l)	GWh	Electricity flow in the line *l*
CURT(t,n)	GWh	Curtailed generation at node *n*
LOSTLOAD(t,n)	GWh	Unsatisfied demand at node *n*
UPSTREAM(t,u)	m^3/s	Inflow from upstream hydro-power plant

The objective function of the problem seeks to minimise the total cost of operating the power system during the simulation period. The total system cost is the result of adding to the variable costs of the different power plants, the cost of pumping, spilling water, transmitting power through the interconnections, curtailing renewable power output, and shedding load.

$$SystemCost = \sum_{t,u} VarCost(u) \cdot G(t,u) + \sum_{t,u} PumpingCost \cdot PUMP(t,u) + \sum_{t,u} SpillageCost \cdot SPILL(t,u) + \sum_{t,l} TransmissionCost \cdot FLOW(t,l) + \sum_{t,n} CurtailmentCost \cdot CURT(t,n) + \sum_{t,n} LostLoadCost \cdot LOSTLOAD(t,n)$$

The objective function is constrained by a set of equations describing the constraints of the WAPP system:

— Market clearing

For each node the supply (i.e. generation and electricity imports) must satisfy the demand plus the curtailment and the unsatisfied load:

$$\sum_{u \in U(n)} G(t,u) + \sum_{l \in L(n)} FLOW(t,l) = Demand(t,n) + \sum_{u \in PUMP(n)} PUMP(t,l) + CURT(t,n) - LOSTLOAD(t,n)$$

— Generation bounds

The energy generated by each unit of any type during the simulation step has to stay within the minimum and the maximum capacity of the unit converted in daily energy generation by multiplying by the duration of the time step in hours:

$$Pmin(u) \cdot 24 < G(t,u) < Pmax(u) \cdot 24$$

— Hydro-power generation

The energy generated by reservoir-based plants is equal to:

$$G(t,u) = \eta(u) \cdot DIS(t,u) \cdot NominalHead(u) \cdot g \cdot density \cdot 3600 \cdot 24/3.6 \cdot 10^{12}$$

Where g is the gravity constant and the other numbers are needed for the conversion of water flow (m^3/s) into energy (GWh).

For run-of-river plants the equation is the same without including the head parameter.

— Wind and solar generation

The energy generated by solar and wind is limited by the capacity factors (provided as inputs) multiplied by the installed capacity.

— Transmission bounds

The electricity flow in each transmission line must be lower than the line capacity.

— Curtailment

For each node the curtailment must be lower than the total production of the units suitable for curtailment, namely hydro-power, wind and solar power.

— Water balance

The water balance in a reservoir is defined by:

$$RES(t,u) - RES(t-1,u) = f1(Inflow(t,u) - Evaporation(t,u) + UPSTREAM(t,u) + CH(t,u) - DIS(t,u) - SPILL(t) - Demand\_Water(t,u)$$

with *f1* defining the conversion factor from m^3/s to hm^3.

— Minimum outflow

The outflow of a hydro-power plant has to be higher than a threshold defined for ecological flow:

$$DIS(t,u) + SPILL(t,u) > Ecological\_flow(t,u)$$

— Maximum spillage

The spillage is bounded by a maximum allowed value:

$$SPILL(t,u) < Spillage\_\max(t,u)$$

— Storage ramping limitations

The reservoirs are assumed to be filled or emptied in 2 months (i.e. 60 days):

$$RES(t,u) - RES(t-1,u) < \frac{Stmax(u)}{60}$$

$$RES(t-1,u) - RES(t,u) < \frac{Stmax(u)}{60}$$

— Storage bounds

The water contained in a reservoir is bounded by the minimum amount of water to be kept in the reservoir and its maximum capacity:

$$Stmin(u) < Res(t,u) < Stmax(u)$$

2.2 The Dispa-SET unit commitment and dispatch module (Dispa-SET UCD)

This module determines the hourly scheduling of the power plants in the modelled power system.

The Dispa-SET UCD model is fully explained in [15][8]. Similar to the Dispa-SET MTHC module, this model can mathematically be written as:

Minimise $C^D(x^D)$

subject to:

$$f^D(x^D) = 0 : (\lambda^D)$$

$$g^D(x^D, z^D, y^{M*}) \leq 0$$

$$x^D \geq 0; z^D \in \{0,1\}$$

where $C^D(\cdot)$ is the system-wide generation cost function, x^D is the vector of continuous dispatching variables, $f^D(\cdot)$ is the function involving all equality constraints, λ^D is the vector of dual variables or Lagrange multipliers associated with the equality constraints, $g^D(\cdot)$ is the function involving all inequality constraints, z^D is the vector of binary commitment variables, and y^{M*} is a given vector of continuous variables in energy units which is the output from the mid-term planning problem.

The unit commitment problem is driven by the system-wide generation cost minimisation, which includes variable and fixed production costs of generating units, start-up and shutdown costs, ramp-up and ramp-down-related costs, and penalisations on some constraints to ensure feasibility.

The unit commitment problem must satisfy technical constraints to provide feasible dispatch and commitment decisions for generating units, i.e. the on/off statuses and the corresponding power productions. The technical constraints that may be considered in the Dispa-SET UCD are listed below:

— Nodal power balance per period.

[8] A full description of this model is available at: http://www.dispaset.eu/en/latest/model.html.

— Power balance in storage units.

— The transmission network, which is represented by a pipeline model, typically used in transport problems.

— Power flow capacity limits.

— Inter-temporal constraints on thermal generators such as ramp-rate constraints or minimum up and down time constraints.

— Storage-related constraints.

— Emission limits.

— Curtailment and load shedding limits.

— Integrality constraints for modelling the on/off statuses of generating units.

— Heating and cooling related constraints.

— Cooling-related constraints for thermal power plants, which are fully explained in the next section.

Due to the binary nature of the commitment decisions, this model is characterised as a large-scale mixed-integer linear program that can be solved by using CPLEX [16] under GAMS [14].

The objective function to minimize is total power system cost, defined as the sum of the following items:

— Fixed costs: depending on whether the unit is on or off.

— Variable costs: stemming from the power output of the units.

— Start-up costs: due to the start-up of a unit.

— Shut-down costs: due to the shut-down of a unit.

— Ramp-up: emerging from the ramping up of a unit.

— Ramp-down: emerging from the ramping down of a unit.

— Load shed: due to necessary load shedding.

— Transmission: depending of the flow transmitted through the lines.

— Loss of load: power exceeding the demand or not matching it, ramping and reserve.

— The variable cost is determined by fuel and emission prices corrected by the efficiency and the emission rate of each unit.

Table 3. List of technologies and fuel codes used by the Dispa-SET model

Technology	**Description**	**Fuel**	**Description**
COMC	Combined cycle	BIO	Bagasse, biodiesel, gas from biomass, etc.
GTUR	Gas turbine	GAS	Natural gas
HDAM	Conventional hydro dam	HRD	Hard coal
HROR	Hydro run-of-river	LIG	Lignite
HPHS	Pumped hydro storage	OIL	Fuel oil and diesel
ICEN	Internal combustion engine	SUN	Solar energy
PHOT	Solar photovoltaic	WAT	Hydro-power
STUR	Steam turbine	WIN	Wind energy
WTOF	Offshore wind turbine		
WTON	Onshore wind turbine		

3 Input data and assumptions

The models applied in the WAPP modelling require a wide range of data as inputs, mostly related to:

— Power plants and interconnections (section 3.1)

— Fuel prices (section 3.2)

— The hourly electricity load (section 3.3)

— The availability of renewable energy sources (section 3.4)

— The water system (3.5)

The quality of a power system model and therefore its usefulness is tightly linked to the quality of the data used as input. To model the WAPP power systems we have used several data sources, listed and described in the following sections. Whenever possible we have cross-checked the data to spot errors and inconsistencies. We are aware of the following limitations in the data we have used for the Dispa-SET modelling:

- The power plant data generally do not include any information on outages and availability of the generation units.
- National electricity demand time-series at daily (or monthly) resolution are not available for most of the African countries, forcing the model to be based on synthetic data (as explained later in Section 3.3)
- No information on operational (e.g. environmental) constraints for hydro-power plants is available for the WAPP.
- In general, time-series of generated power from power plants (thermal and hydro) are not available. Moreover, except for a very few cases (the largest plants in Nigeria and Ghana for example), there are no information on inflows and outflows of large reservoirs.
- There is no information on water use for multi-purpose reservoirs, the only possibility in this case is to rely on model data as explained in Section 3.5.3.

The rest of this section explains the methodology and the publicly available data used to generate all the inputs needed by the models.

3.1 Power system infrastructure

3.1.1 Power plants

A complete list of the power plants available in the WAPP is provided by ECOWREX, the ECOWAS observatory for Renewable Energy and Energy Efficiency. The full list of the 346 power plants[9] has been then compared and completed with the following open sources: the WRI Global Power Plant Database[10] and the ENERGYDATA.INFO open data platform[11]. Those open data have been compared with the commercial S&P Global Platts World Electric Power Plants Database[12] and the reports available on the websites of the WAPP and the national electric utilities in order to find any important inconsistencies. As a result, the input data used for this study are entirely based on open sources.

Particular attention has been given to hydro-power plants due to their importance in this analysis and in general in the supply of electricity in the WAPP region.

[9] Available at: http://www.ecowrex.org/resources/energy_generators.
[10] Available at: http://datasets.wri.org/dataset/globalpowerplantdatabase.
[11] Available at: https://energydata.info.
[12] Available at: https://www.spglobal.com/platts/en/products-services/electric-power/world-electric-power-plants-database.

For each hydro-power plant its characteristics (head, maximum stored water amount and area of the reservoir) have been cross-checked across several sources: the databases above mentioned, data from the Global Energy Observatory[13] (GEO), Global Reservoir and Dam (GRanD) Database[14], river basins authorities (e.g. Volta River Authority), national master plans (e.g. Nigerian National Water Resources Master Plan[15]).

Scientific publication and reports have been also taken into account to obtain and compare information related to power plants and hydrology in Western African countries. Here the list of the most important papers grouped by geographic area:

— Volta basin and hydro-power in Ghana: [17]–[21]

— Nigerian hydro-power: [22]–[32]

— Solar power in Mali: [33]

The area of water reservoirs plays an important role when estimating the evaporation (see Section 3.5.2) and when the information was not available in the above mentioned databases we have used the following sources:

— The WAPP Environmental and Social Impact Assessment (ESIA) and Resettlement Action Plan for the Mount Coffee plant in Liberia[16]

— The Environmental and Social Impact Assessment (ESIA)[17] for the Bui Hydropower Project in Ghana

— Copernicus satellite imagery available from EO Browser[18] for Kwall (Nigeria), Kpime (Togo), Kinkon (Guinea), Kaleta (Guinea), Kurra (Nigeria), Jekko (Nigeria), Guma (Sierra Leone)

— The Nigerian National Water Resources Master Plan for Nigerian hydro-power plants[19]

— The paper [34] for Kompienga and Bagre in Burkina Faso

3.1.2 Grid infrastructure

A geo-localised dataset with the existing and planned transmission lines is provided by the WAPP GIS database[20]. The dataset does not contain the transfer capacities, which have been obtained comparing different sources:

— The report [35] on West Africa

— The scientific paper [36], [37] on the African electricity supply sector

— Report of regional authorities: Commission de Régulation de l'Electricité et de l'Eau in Mali[21]

3.2 Fuel prices

In this work we have considered the fuel prices from two sources: the IRENA report on West Africa [35] and the WAPP Master Plan[22].

[13] Available at: http://globalenergyobservatory.org/.
[14] Available at: http://www.gwsp.org/products/grand-database.html.
[15] Available at: http://open_jicareport.jica.go.jp/pdf/12146569.pdf.
[16] Available at: http://www.eib.org/attachments/pipeline/20120342_esia_en.pdf (accessed 19-12-2018)
[17] Described here: https://www.buipower.com/node/142 (accessed 19-12-2018) and available at: http://library.mampam.com/Final%20ESIA%20-%20Bui%20HEP.pdf
[18] Available at: https://apps.sentinel-hub.com/eo-browser/
[19] Available at: http://open_jicareport.jica.go.jp/pdf/12146478_03.pdf (accessed 19-12-2018)
[20] Available at: http://www.ecowrex.org:8080/geonetwork/srv/eng/catalog.search#/metadata/2e031279-18fd-4ac9-8ba9-fadf3d97651f.
[21] See for example the report available at http://www.creemali.ml/documents/RAPPORT_CREE_2014.pdf (accessed 19-12-2018)
[22] See Section 3.1.2 in the Volume 1 of "Update of the ECOWAS revised master plan for the generation and transmission of electrical energy" available at: http://www.ecowapp.org/sites/default/files/mp_wapp_volume_1.pdf (accessed 19-12-2018)

Table 4. Fuel prices used in this study

Fuel	Cost (USD/MWh)
Oil/Diesel – coastal	79.1
Oil/Diesel – inland	91.1
Natural gas - domestic	50.1
Natural gas – pipeline	60.7
Natural gas – imported	64.9
Coal – domestic	23.3
Coal – imported	34.6
Biomass – moderate	11.3
Biomass – scarce	27.5

Table 4 provides a summary of the fuel prices (in USD per MWh, the currency used in the data sources used for this analysis) used in this study. For the various fuel types we distinguish according to the typology of supply for each country:

- Oil/Diesel: Burkina Faso (BFA), Mali (MLI) and Niger (NER) are considered "inland" while the rest of the countries are "coastal".
- Natural gas: Ivory Coast (CIV), Nigeria (NGA) and Senegal (SEN) are classified as "domestic"; Benin (BEN), Togo (TGO) and Ghana (GHA) as "pipeline" and the rest are "imported".
- Coal: only Niger (NER) and Nigeria (NGA) are classified as "domestic", the rest are "import".
- Biomass: Burkina Faso (BFA), Niger (NER) and Mali (MLI) are considered having a "scarce" availability, while the rest is classified as "moderate".

3.3 Hourly load profiles

3.3.1 Available historical load profiles

The modelling framework described to analyse the water-power nexus needs hourly inputs describing the electricity demand in the different countries. Due to the lack of historical data, the hourly load profiles fed into the models for this analysis are estimated from the available energy statistics combined with meteorological data.

In the case of the load, IRENA provides profiles only for Ghana (2009), Ivory Coast (2008) and South Africa (2010)[23] while the BETTER project[24] provides the 2010 profiles for Algeria, Egypt, Libya, Morocco and Tunisia. The available energy data for the rest of African countries is provided in aggregated form by the IEA[25] and the African Energy Commission[26].

[23] http://www.irena.org/SAPP.
[24] Deliverable 3.2.1 "Demand Development Scenarios", available at: http://better-project.net/.
[25] World Energy Statistics and Balances: https://www.iea.org/classicstats/relateddatabases/worldenergystatisticsandbalances/.
[26] https://afrec-energy.org/En/index.html.

Figure 2. Hourly load profiles, averaged with annual load

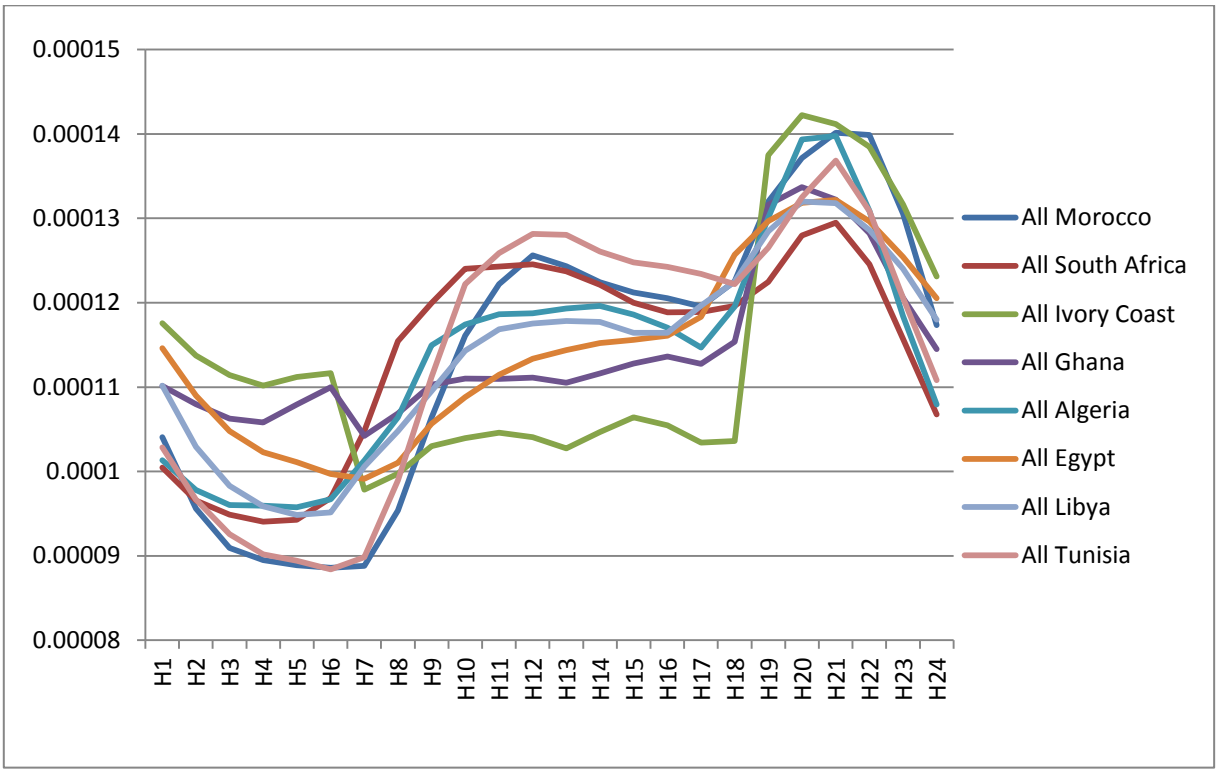

Figure 3. Hourly load profiles, ratio of hourly to daily average

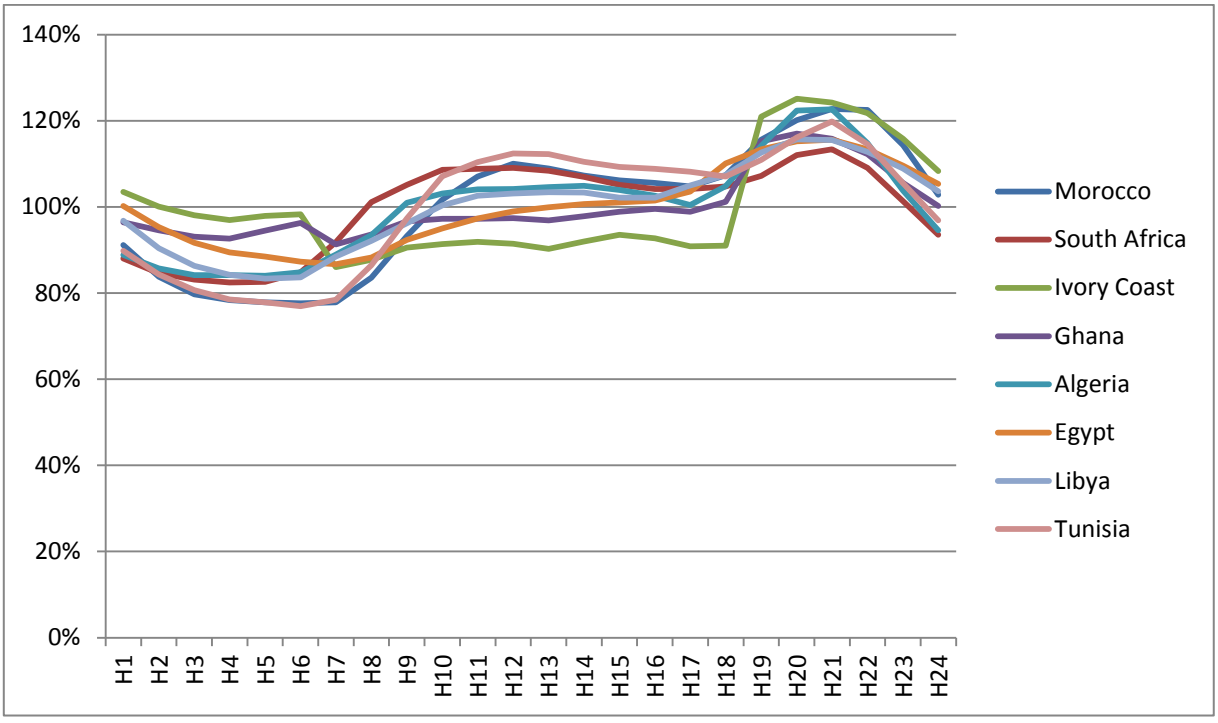

3.3.2 Estimation of the synthetic hourly load profiles

The hourly load profiles are estimated in two steps: i) the normalised final electricity consumption is calculated by means of Multiple Linear Regression (MLR) as a function of the final electricity demand in different sectors and meteorological variables, and ii) the normalised final electricity consumption is then combined with the annual electricity consumption, the

losses, and the own use in the energy industry (all obtained from the available energy statistics) to derive the hourly load.

There are several statistical techniques extensively used to forecast hourly load profiles. Recently, some studies have shown that the best performing ones are those based on time series analysis. In particular, [38] and [39] showed that exponential smoothing models for double seasonality (D-SARIMA) have the best performance for the case of Spain. They confirmed the D-SARIMA models were the best and they also demonstrated that the inclusion of the electricity load and wind generation forecasts provided by the TSOs significantly improve the predictive capabilities of the forecasting methods in the Spanish electricity market. However, these techniques are based on the analysis of the evolution over time of the variable of interest (in this case, the load). In this case the purpose of the analysis is to find a model which allows identifying the dependency of the forecasted variable (load) as a function of the deviations of different quantitative (different types of consumption and meteorological variables) and temporal variables (seasonality, day and night, working days and weekends, etc.). Thus, a Multiple Linear Regression (MLR) model is applied because of being a well-known and robust technique suitable for achieving this objective.

Under the MLR approach, the selection of the explanatory variables is a key issue because irrelevant or noisy variables have negative effects on the training process. Therefore, a principal component analysis (PCA) is applied for internal consistency assessment and to check to what extent indicators within the same component measure the same latent variable. Internal consistency, which is related to the level of correlation or association amongst indicators, if established, reduces the effect of different weighting schemes on the final, aggregated measure. In addition, to ensure that the MLR approach is the suitable methodology, it has been tested so that the input variables selected are linear (all of them follow a normal distribution) and independent from each other.

The independent variables selected to simulate the normalised final consumption of electricity in each hour are the following:

— **Hour**: the time of day, from 1 to 24

— **Season**: the quarter of the year (Q1 from hours 1 to 1416 and from 8041 to 8760, Q2 from hours 1417 to 3624, Q3 from hours 3625 to 5832, and Q4 from hours 5833 to 8016).

— **Day and night (D.N)**: from 09:00 to 18:00, when commercial and public services are supposed to operate.

— **Labour day / Weekend (LabDay)**: Monday to Friday vs. Saturdays and Sundays.

— **Consum_indu_rest**: final energy consumption in industry (except construction), split equally during all hours.

— **Consum_indu_cons**: final energy consumption in construction, split equally during commercial hours.

— **Consum_trans_rest**: final energy consumption in transport (except pipelines), split equally during commercial hours.

— **Consum_trans_pipe**: final energy consumption in pipeline transport split equally during all hours.

— **Consum_other_rest**: final energy consumption in agriculture, forestry, fishing and non-specified sectors, split equally during all hours.

— **Consum_other_resi**: final energy consumption in the residential sector, split equally during commercial time and during morning (10:00-14:00) and evening (19:00-23:00) peaks.

— **Consum_other_pub**: final energy consumption in commercial and public services, split equally during commercial hours (09:00-18:00).

— **Meteorological variables**: Solar PV (PVpower), irradiance (Irradiance), sun height (sunheight), temperature (Air_temp), wind speed (Wind_speed) are hourly time series

(from 1 to 24) averaged over each country for the year 2010. The source of the data is explained in section 3.4.

3.3.3 Model performance

This PCA/MLR technique has been applied to all the African countries with historical load hourly available data. A predictive-model based approach has been defined for those countries. To obtain hourly load profiles for the remaining countries with no available historical load data, the predictive-model of the neighbour country with available data has been applied, as specified in Table 5.

Table 5. Modelled countries

Historical profile	**Modelled country**
Algeria	Algeria
Egypt	Egypt
Ghana	Angola, Benin, Botswana, Burkina Faso, Burundi, Cameroon, Central African Republic, Chad, Congo, Democratic Republic of Congo, Ivory Coast, Djibouti, Equatorial Guinea, Eritrea, Ethiopia, Gabon, Gambia, Ghana, Guinea, Guinea-Bissau, Kenya, Lesotho, Liberia, Madagascar, Malawi, Mali, Mauritania, Mauritius, Mozambique, Namibia, Niger, Nigeria, Rwanda, Senegal, Sierra Leone, Somalia, South Sudan, Swaziland, Tanzania, Togo, Uganda, Zambia, Zimbabwe
Libya	Libya
Morocco	Morocco, Western Sahara
South Africa	South Africa
Tunisia	Tunisia

For example, for Morocco, the PCA analysis shows that the variables selected to build the MLR model accounts for 99.99% of the variability in the dataset Table 6. The first principal component (PC), explaining 99.86% of the variability, is a combination of all the variables included (although in this particular case, *Consum_indu_rest*, *Consum_trans_rest*, *Consum_trans_pipe* and *Consum_other_rest* have insignificants weights with respect to the other variables). In the second component, the main variability is also due to all the input variables selected, which explain 0.06% of the variability. Note that since the purpose of this study is to evaluate the impact of the meteorological and temporal variability and the consumption clustered in different sectors, all the variables plays an important role in defining the load features although some of them will not add significant variability (such as the *Consum_indu_rest*, *Consum_indu_cons*, *Consum_trans_pipe* and *Consum_other_rest*). The PCA analysis gives 14 principal components explaining the 100% load variability. However, in this case, the first PC is the most significant explaining the 99% of the total load variability. Therefore the PC1 is selected for the regression technique to forecast the load.

Table 6. First and second Principal Components for the Morocco case study

Variable and acronym	PC1	PC2
Hour (hour)	1.381	40.811
Season (Season)	1,55E+02	2,25E+04
Day and night (D.N)	8,56E+02	1,03E+04
Labour day / Weekend (LabDay)	-2,07E+01	6,85E+02
Consum_indu_rest	-5,17E-20	-6,94E-12
Consum_indu_cons	1,65E-35	1,21E-33
Consum_trans_rest	1,60E-03	1,99E-02
Consum_trans_pipe	0	1,06E-16
Consum_other_rest	0	-8,27E-19
Consum_other_resi	4,30E-03	4,51E-02
Consum_other_pub	5,26E-02	1,98E-01
Solar PV (Pvpower)	6,28E+05	-5,81E+05
Irradiance (Irradiance)	7,77E+05	4,29E+05
Sun height (sunheight)	4,67E+04	6,58E+05
Temperature (Air_temp)	6,79E+03	2,07E+05
Wind speed (Wind_speed)	3,15E+02	-1,23E+04

Following the analysis of the best MLR model performances by [40]; a linear stepwise regression is applied, with interaction terms following the Sawa's Bayesian Information Criteria (INT-BIC). For each of the independent variables, the F-statistic is calculated to determine each variable's contribution to the model. The stepwise regression evaluates all of the variables already included in the model and removes any variable that has an insignificant F. That estimates a measure of the difference between a given model and the "true" underlying model. The model with the smallest BIC amongst all competing models is deemed the best model. Here, the BIC is a function of the number of observations (n), the sum of square errors (SSE), the pure error variance fitting the full model (σ^2), and the number of independent variables ($k \leq p + 1$) where k includes the intercept) where k includes the intercept to measure the forecast accuracy.

$$BIC = \mathrm{n} + \ln\left(\frac{SSE}{n}\right) + \frac{2(k+2)n\sigma^2}{SSE} - \frac{2n^2\sigma^4}{SSE^2}$$

The model is built selecting different periods: the training and the testing dataset. This process has been carried out different times (each time considering one different period over the 2010 year for the testing period), and after the convergence of finding the best R^2, the best model resulting from the iterations is selected.

$$
\begin{aligned}
&Normalised\ Final\ Electricity\ Consumption(Country, Hour) \\
&\quad = k + [\alpha_1 \cdot hour] + [\alpha_2 \cdot \text{Season}] + [\alpha_3 \cdot \text{D.N}] + [\alpha_4 \cdot \text{Labday}] + [\alpha_5 \cdot Consum\_indu\_rest] \\
&\quad + [\alpha_6 \cdot Consum\_indu\_cons] + [\alpha_7 \cdot Consum\_trans\_rest] + [\alpha_8 \cdot Consum\_trans\_pipe] \\
&\quad + [\alpha_9 \cdot Consum\_other\_rest] + [\alpha_{10} \cdot Consum\_other\_resi] + [\alpha_{11} \cdot Consum\_other\_pub] \\
&\quad + [\alpha_{12} \cdot \text{Pvpower}] + [\alpha_{13} \cdot \text{Irradiance}] + [\alpha_{14} \cdot \text{Sunheight}] + [\alpha_{15} \cdot \text{Air\_temp}] \\
&\quad + [\alpha_{15} \cdot \text{Wind\_Speed}] + \varepsilon
\end{aligned}
$$

The hourly load is then estimated as the product of the annual electricity consumption (augmented by the annual losses and the own use in the energy industry, from the energy statistics) and the absolute values of the normalised final electricity consumption (computed as the ratio of the normalised final electricity consumption to its sum throughout the year, to denormalise):

$$
\begin{aligned}
&Hourly\ load(Country, Hour) \\
&\quad = Annual\ electricity\ consumption \cdot (1 + Annual\ Losses + Annual\ Autoconsumption) \\
&\quad \cdot \frac{Normalised\ Final\ Electricity\ Consumption(Country, Hour)}{\sum_{(Country, Hour)} Normalised\ Final\ Electricity\ Consumption(Country, Hour)}
\end{aligned}
$$

Generally, it is considered that a good linear model has a small RMSE and a high adjusted coefficient of determination (R^2) close to 1, verified in the testing period. These coefficients evaluate the degree of agreement between modelled vs. observed load. R^2 is the square of the correlation coefficient (R).

Table 7. Coefficients of the model-based load hourly profiles for Morocco

Variables	Coefficients	Std. Error	tvalue	Pr(>|t|)	Significance[27]
(Intercept)	-7,55E-03	1,18E-03	-6.430	1.34e-10	***
hour	3,48E-05	2,89E-05	1.207	0.2276	
Season	2,08E-04	1,12E-04	1.860	0.0629	.
D.N	-1,22E-02	4,72E-04	-25.824		***
LabDay	-1,59E-03	5,06E-05	-31.327		***
Consum_indu_rest	NA	NA	NA	NA	
Consum_indu_cons	NA	NA	NA	NA	
Consum_trans_rest	1,46E+03	1,33E+02	10.964	<	***
Consum_trans_pipe	NA	NA	NA	NA	
Consum_other_rest	NA	NA	NA	NA	
Consum_other_resi	2,26E+03	3,18E+01	70.912		***
Consum_other_pub	4,69E+01	8,80E+00	5.334	9.85e-08	***
Pvpower	4,24E-05	1,02E-05	4.173	3.04e-05	***
Irradiance	-4,03E-05	8,43E-06	-4.776	1.82e-06	***
sunheight	3,15E-05	1,36E-05	2.312	0.0208	*
Air_temp	1,90E-03	3,52E-05	54.023		***
Wind_speed	-1,21E-03	7,29E-05	-16.586		***

Table 7 presents the coefficients of the equations. The "residuals" give the difference between the experimental and predicted signals. The estimates for the model's coefficients are provided along with their standard deviation ('std Error') as well as the t-value and probability for a null hypothesis that the coefficients have values of zero. At the bottom of the table is the standard deviation about the regression (residual standard error). An F-test result on the null hypothesis (F-statistic = 3066 on 12 and 8747 degrees of freedom) with the correlation coefficient (R = 0.89) of the model is also included in the analysis. Where intercept is the constant value of which e is the residual and αi are the coefficients for each independent variable.

3.3.4 Statistical validation and benchmarking with existing sources

The overall results of the statistical performance for each country with available historical data are summarising in Table 8. The fractional bias (FB) measures the mean bias and indicates only systematic error which leads to an underestimation or overestimation (in the range of

[27] The significance codes are 0 '***' 0.001 '**' 0.01 '*' 0.05 '.' 0.1 ' ' 1. The residual standard error is 9.431e-06 on 8747 degrees of freedom (DF). Multiple R2 0.8079, adjusted R2 0.8077. F-statistic I 3066 on 12 and 8747 DF. P-value < 2.2e-16 (***)

±2.0 ratio) of the historical values. There are no significant differences between the FB associated to the simulated values by country.

A tendency to underestimate is found in some countries while in Libya is overestimated, but in all countries is very low. The Pearson's linear correlation coefficient indicates that the simulations have a good internal consistency, they range between 0.65 – 0.90. In addition, the mean error (ME), the difference between standard deviations (SD) and the root mean square error and the unbiased root mean square error (RMSE and $RMSE_{ub}$) are computed to gauge the simulation's accuracy. Indeed, high values of $RMSE_{ub}$ indicate a high level of non-systematic (i.e., random) discrepancy between the simulations and the historical data. In addition, the ability of a simulation to reproduce the "real" values is also assessed following the criteria defined by [41] consisting of: (1) the simulated and historical standard deviations are similar; (2) the RMSE are lower than the standard deviation and (3) the unbiased RMSE ($RMSE_{ub}$) which represents the accuracy of the simulated load is also lower than the standard deviation.

$$FB = \frac{\sum_i (Xi_{obs} - Yi_{simu})}{0.5 * \sum_i (Xi_{obs} + Yi_{simu})}$$

$$ME = \frac{\sum X_i - Y_i}{n}$$

$$SD = \sqrt{\frac{\sum_{i=1}^{n} (X_i - \overline{X})^2}{n-1}}$$

$$RMSE_{ub} = \sqrt{\frac{\sum_{i=1}^{n} ((X_i - \overline{X}) - (Y_i - \overline{Y}))^2}{n}}$$

Table 8. Statistical parameters to gauge the performance of the model for load hourly profiles

Statistics	South Africa	Morocco	Algeria	Egypt	Libya	Tunisia
FB	-0.0264	-0.0091	-0.0210	-0.0156	0.0172	-0.0968
R^2	0.90418	0.8988	0.7661	0.8740	0.6571	0.8524
SD_{obs}	3.4979	0.5918	0.8465	2.3425	0.6915	0.3545
SD_{simu}	3.5901	0.5367	0.6226	2.0193	0.4476	0.3284
ME	0.7654	0.0287	0.1086	0.2604	-0.0643	0.1718
MSE	3.0007	0.0681	0.3084	1.3640	0.2758	0.0645
RMSE	1.7322	0.2610	0.5553	1.1679	0.5252	0.2541
$RMSE_{ub}$	1.5539	0.2541	0.5446	1.1385	0.5212	0.1872

Figure 4 shows the quality of agreement between the load simulated and historical datasets in the form of Taylor diagram for the same countries validates. Those diagrams assess comparatively the modelled and observed data by the use of the Pearson correlation coefficient, the root mean square error and the standard deviation. The normalised standard deviation and the correlation is higher for South Africa (1 and 0.9, respectively) following by Morocco, Tunisia and Egypt with similar results. Algeria and Libya have lower values but still good enough to reproduce the load profiles.

Figure 4. Taylor diagram for visualising the statistical significance of the model performance

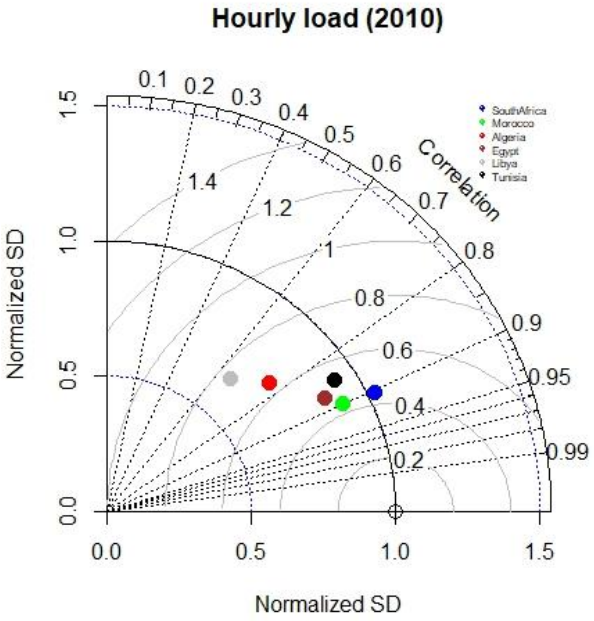

The simulated time series of the load have been compared with the real load generation data for the year 2010. The figure below shows an example of the load (simulated – coloured in red - against the real – coloured in blue - load time series) for Morocco (Figure 5).

Figure 5. Comparison of the simulated and real load hourly time series (in MW) for Morocco

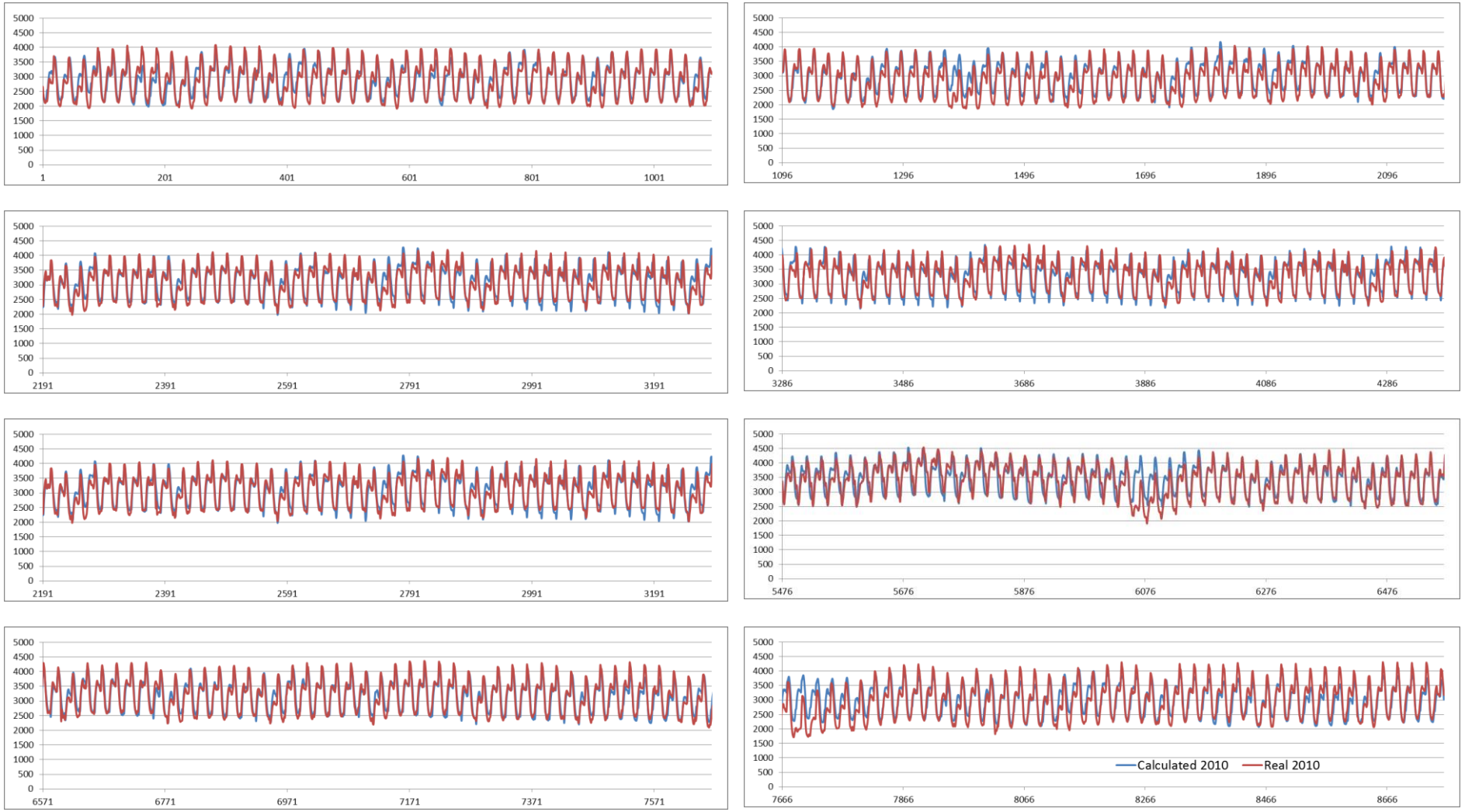

For benchmarking with existing sources of load profiles, one attempt has been found carried out by Krutova et al. [42] aiming at analysing the smoothing effect of the RES-E resources at Afro-Eurasian power grid. Since the purpose of that study was at global scale, they simplified the power network covering large parts of Eurasia and Africa. They clustered the countries from Northern Africa (NA) as: Algeria, Egypt, Libya, morocco and Tunisia and they released one single time series for the country of South Africa. Thus, to make a preliminary comparison for the load profiles with Krutova et al. both the 2010 historical data and the data generated in EMHIRES-Africa are equally grouped as "NA" and South-Africa. A comparatively analysis and Pearson's correlation coefficient (R) show that the load data from this study is far from the historical record while EMHIRES hovers around 90% of correlation.

Table 9. Pearson 'correlation coefficients and summary of statistics for load hourly profiles between historical load profiles, EMHIRES-Africa and Krutova et al.

		REAL	**EMHIRES**	**KRUTOVA**
South Africa	**HISTORICAL**	1	0.904	0.347
	EMHIRES		1	0.338
	KRUTOVA			1
		REAL	**EMHIRES**	**KRUTOVA**
North Africa	**HISTORICAL**	1	0.876	-0.112
	EMHIRES		1	-0.063
	KRUTOVA			1

Table 10. Statistical comparison between EMHIRES –Africa dataset and Krutova et al.

	HISTORICAL		**EMHIRES**		**KRUTOVA**	
STATS	**North Africa**	**South Africa**	**North Africa**	**South Africa**	**North Africa**	**South Africa**
Min.	20.9	19.72	21.86	21.67	34.45	5.418
1st. Qu	27.05	25.28	28.09	25.79	53.77	11.482
Median	29.69	29.22	30.58	30.53	64.42	14.008
Mean	30.2	28.59	30.71	29.35	64.34	14.015
3rd. Qu	33.56	31.41	33.46	32.28	74.79	16.623
Max.	41.7	37.24	40.16	35.87	95.43	22.352

3.4 Wind and solar PV generation

3.4.1 Wind resource data

In this study, the wind speed data are obtained from the ERA5[28] reanalysis data. ERA5 makes wind speed data (two horizontal velocity components) available at a number of pressure levels in the atmosphere, but also at 10m and 100m above the ground. These two altitude levels have been used to calculate the wind speed at 50 m height, the assumed average hub height. ERA5 is the first reanalysis produced as an operational service and provides data at a considerably higher spatial and temporal resolution: hourly analysis fields are available at a horizontal resolution of 31 km, and on 137 levels from the surface up to around 80 km. In addition, information on uncertainties is provided for each parameter at 3-hourly intervals and at a horizontal resolution of 62 km. The region covering Africa is (N: 40N; S: 35S; W: 25W; E: 60E) interpolated to the horizontal resolution at 15' (~28km), which is close to the native resolution of ERA5.

3.4.2 Solar resource data

The solar PV time series generated come directly from the PV GIS model[29]. In this model, solar radiation data have been obtained from satellite-based algorithms. The data are available as the SARAH Climate Data Record from the CM SAF collaboration[30]. The solar radiation data include both the global horizontal and direct horizontal irradiance; this makes it possible to calculate the irradiance on inclined planes, which is the typical configuration for PV modules. The time resolution of the solar radiation data used for this study is hourly, and the spatial resolution is 3 arc-minutes (about 5km). Air temperature (at 2m above ground) is used for modelling the instantaneous PV output extracted from ECMWF ERA5 reanalysis. Note that the relatively coarse resolution could lead to errors in mountainous areas with large variations in elevation or near the coastlines.

PV arrays are generally mounted at an angle from horizontal, both to increase the amount of solar radiation reaching the modules, and to reduce soiling (dust deposition) by allowing rainwater to clean the modules The inclined-plane irradiance is estimated using different models to account for the increased reflectance at the module surface when the light arrives at an oblique angle to the module surface. Together, these two models yield the effective irradiance, i.e. the solar irradiance arriving at the PV cells in the module. All abovementioned configuration and the PV output power is calculated following [43], which describe the PV power as a function of in-plane irradiance and module temperature. The coefficients used for modelling crystalline silicon PV modules are also taken from the same study.

3.4.3 Estimation of the RES profiles

The wind and solar resource data are used for estimating the availability factors of wind and solar generation units. The general approach to convert wind and solar resource time series into power consists in converting the wind speed and radiation data from weather models or observations using different types power curves. The power curves, which are also technology dependent, provide the value of electrical power output as a function of wind speeds and radiation (at the hub height for the case of the wind energy).

Figure 6 schematically explains the first step (from wind and solar resources to power generation). The wind power output is generated using the EMHIRES-wind methodology [44]. The model uses historical data based on ancillary meteorological data from reanalysis to calculate the power from the wind fleet. The technological aspects (such as the power curves, turbine types, geographical locations of the wind farms) are taken

[28] https://www.ecmwf.int/en/forecasts/datasets/archive-datasets/reanalysis-datasets/era5
[29] http://re.jrc.ec.europa.eu/pvgis/apps4/pvest.php
[30] https://www.cmsaf.eu/EN/Home/home_node.html.

from a JRC internal reconstructed and gap-filled dataset [45], which is based on available studies.

The PVGIS model provides PV power output estimates at high temporal and spatial resolution for the entire study area. PVGIS combines satellite-based solar radiation data with climatic data (especially temperature and wind speed) and with mathematical models for PV system performance to produce time series of PV power production over large regions with hourly time resolution and a spatial resolution of a few km. If necessary, the effect of shadows from local terrain features is also be taken into account. The PV production data is then spatially aggregated when needed.

Figure 6. Method used to generate the RES-E dataset and load profiles

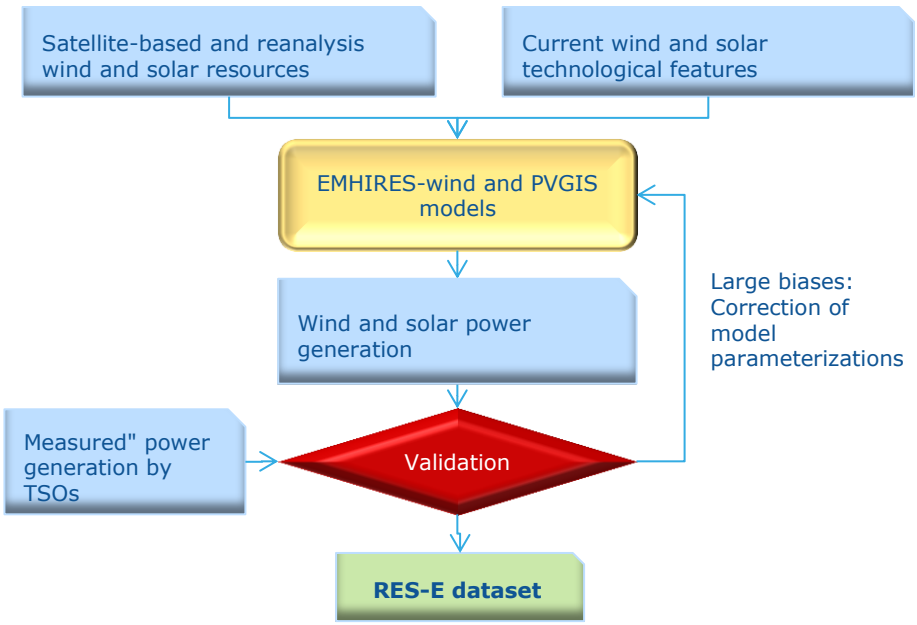

For the case of solar PV time series, the PV output (W/ KWp) obtained from the PV GIS model follows several assumptions: the inclination is equal to the latitude, with a minimum slope of 10 degrees equator-facing (so north-facing in the southern hemisphere). For the first release of the solar PV generation time series over Africa, it is considered that the PV portfolio is placed in one single location for each country at the capital city. That would be representative of one or a few large PV installations in that location, but if the PV arrays are more spread-out in the country the aggregated time series for the country will change (smoother). In general, in many countries over Africa it is possible to assume that PV systems would be nearly everywhere, but of course in sparsely populated places like Namibia or Chad it would maybe be better to assume that PV power plants would be not too far from population centres. Then, once again, sparsely populated normally means desert, so the PV power is likely to be nearly the same everywhere since there are few clouds.

Similarly, for the case of wind power, in the first version released, the wind speed is aggregated at national level, considered the capital city as a main location of the wind portfolio. The first approach to immediately convert the wind speed per African country into power is to use average wind turbine type – wind power curve (extracted from the average wind turbines registered in our databases). The typical wind turbine considered here is Vestas (V90 – 2MW) at a 50 m height. The national aggregated values have been compared with the JRC internal wind farm database, which is a combination of commercial and publicly available datasets, at global, continental and national levels.

This is an approximation for calculating the wind power generation in each country. For a more precise methodology several additional factors are needed, such as:

— Specific locations of the wind farms, to extract the wind speed at each wind farm site.

— Density corrections, both for elevation and air temperature.

— More detailed technology of each wind farms of the country, to apply the corresponding technological power curve for each wind farm.

The first version of the wind and solar PV generation hourly time series covers a period ranging from 1 January 2005 to 31 December 2016, given at national levels.

3.4.4 Benchmarking with other estimations

As mentioned in the introductory section, there are no available source of wind and solar power hourly time series for the African continent estimating the generation with the current portfolio. However, to further test the validity of our wind and solar power time series we compare it with the renewables.ninja[31] dataset, which is based on the similar hypotheses such as aggregation level, technology, inclination plane for the case of solar PV. The results show high correlations between the two datasets for the African countries: on average at the African continent, correlations of 0.80 and 0.70 for the solar and wind power time series in 2010, respectively. The table below shows the example of wind and solar power time series correlations for Algeria and South Africa, indicating that although the hypotheses are not the same, both datasets show consistent results.

Table 11. Comparison between EMHIRES –Africa Renewables.ninja wind and solar power time series (2010)

CORRELATIONS			**EMHIRES**			
			PV	**WIND**	**PV**	**WIND**
			ALGERIA		**SOUTH-AFRICA**	
NINJA	**PV**	**ALGERIA**	**0.901**	0.149	0.564	0.064
	WIND		-0.103	**0.721**	0.100	-0.028
	PV	**SOUTH-AFRICA**	0.681	0.071	**0.701**	0.134
	WIND		-0.114	-0.078	-0.155	**0.702**

3.5 Water system assumptions

3.5.1 Inflows

Considering the importance of hydro-power generation in the WAPP area, the definition of realistic inflows was fundamental. Unfortunately, river discharges observations are very limited as well as the availability of statistics that could be of any use to implement a simulation at daily or hourly scale. For this reason a hydrological model operated by the JRC has been used to generate all the data we needed consistently and at high-resolution for a long time period. The LISFLOOD model, a hydrological rainfall-runoff model, was capable of simulating the hydrological processes occurring on the target area. The model has been developed by the floods group of the Natural Hazards Project of the JRC [12] and it has generated a gridded inflow with 10 km of resolution for the period 1979-2010. Then, for each hydro-power plant we have extracted a daily inflow from the nearest grid point according to its coordinates.

[31] https://www.renewables.ninja/

The inflow time-series have been then calibrated by using the data produced by the hydropower resource mapping from ECOWAS[32]. In the ECOWAS report, a very detailed model of the Western African river network based on model outputs, satellite data and about 800 stream gauges, has been produced, with a set of monthly statistics about river flows for each river section. The correction procedure we have implemented is based on calculating for each month the delta between the LISFLOOD average river flow and the ECOWAS river network. Then this monthly delta has been used to correct the daily LISFLOOD inflows used as inputs in the Dispa-SET model.

The inflows used in the Dispa-SET model as described in Section 4 are shown in Figure 7. The figure presents the inflows for all the hydro-power plants modelled by Dispa-SET based on the output of the LISFLOOD model for the years 1979-2010.

[32] Available at: http://www.ecowrex.org/sites/default/files/final_technical_report_on_methodology_and_lessons_learnt_for_ecowas_countries.pdf (accessed 19-12-2018)

Figure 7. Calibrated inflows used for the modelled hydro-power plants for the years 1979-2010. The blue line shows the multi-annual mean.

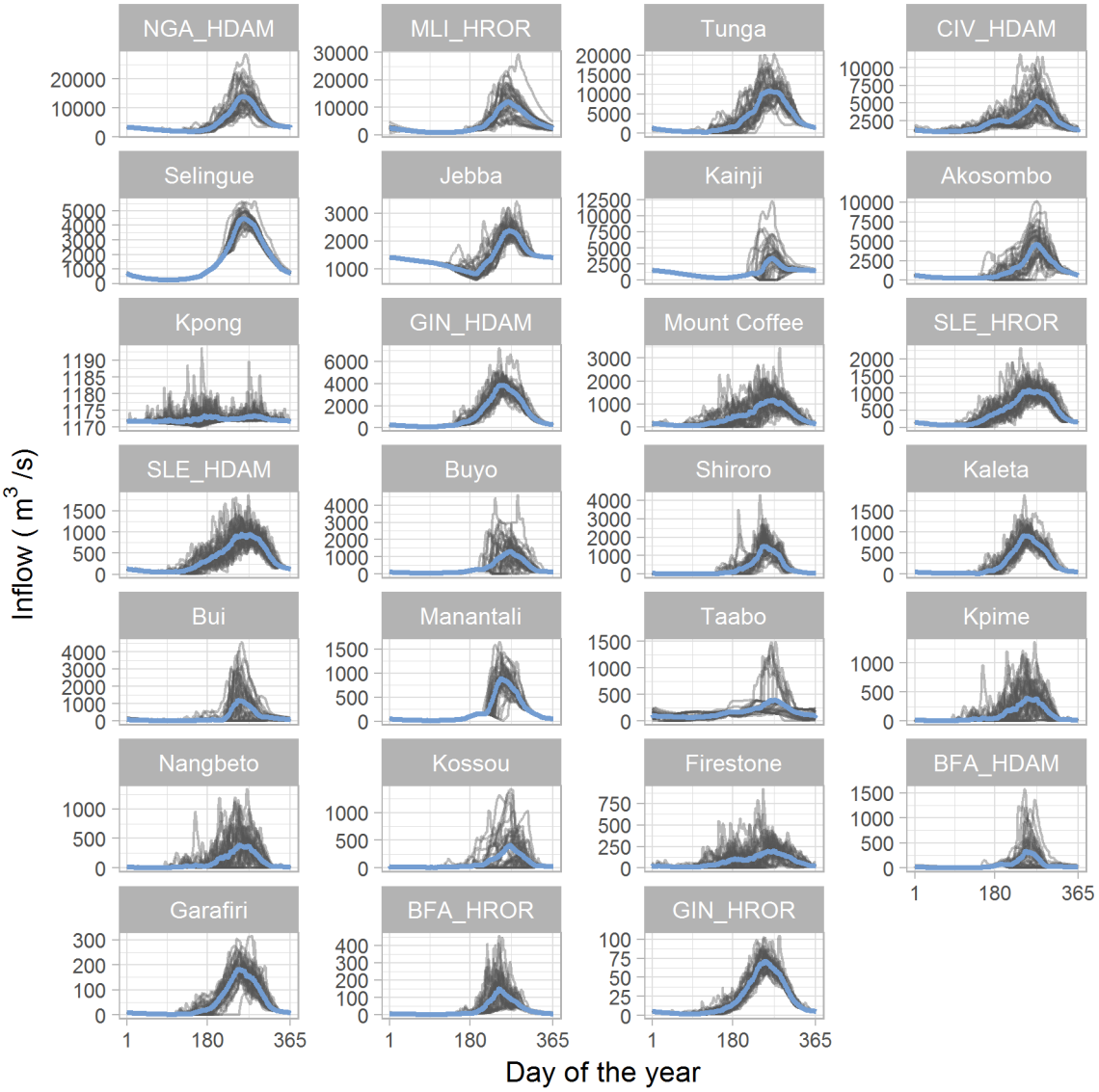

3.5.2 Evaporation

The amount of water lost due to evaporation may be very high, for example according to [46] the Akosombo reservoir in Ghana loses only for reasons of evaporation 2 meters per year, a water quantity corresponding to half of the capacity of entire Volta River (where the reservoir is located). To take evaporation into account, we have used the routines implemented in the "evapotranspiration" package developed in R[33]. We use the Hargreaves-Samani formulation [47]–[49] which estimates the daily evapotranspiration from the elevation in meters and the maximum and minimum daily temperatures. The elevation data has been obtained from the TerrainBase (TBASE) dataset[34] from the National Center for Atmospheric Research (NCAR), the temperature data is instead from the ECMWF ERA-INTERIM reanalysis [50].

The Hargreaves-Samani formula has been then applied using for each reservoir the nearest grid point for the elevation and temperature data sets.

[33] The package is available on the official R archive: https://CRAN.R-project.org/package=Evapotranspiration
[34] Available at: http://research.jisao.washington.edu/data_sets/elevation/

Whenever possible, our estimations have been compared with data available on official sources [46].

3.5.3 Water demand

Some of the reservoirs in the area targeted by this study are multi-purpose, thus the water is used not only for electricity generation but also for irrigation, domestic use, etc. To estimate the water withdrawal we have used the open dataset described by Huang et al. [51][35]. The dataset is gridded (0.5 degree of spatial resolution), with monthly resolution, and it was generated using a set of different models for the following sectors: irrigation, domestic use, livestock, manufacturing, mining and electricity generation.

We have selected a set of reservoirs for which we have estimated the amount of water withdrawal for each month for irrigation, livestock, domestic use and manufacturing. The estimation followed a very simple procedure:

1. For each reservoir we consider an area of about 25 000 km^2 surrounding the reservoir (the cell including the reservoir and the 8 surrounding grid cells)
2. We sum all the water withdrawal in the area from the dataset for the selected grid cells
3. We interpolate linearly the water demand from monthly to daily frequency

[35] The dataset can be downloaded at the following URL: https://doi.org/10.5281/zenodo.897932

4 Case study: the West African Power Pool

This section presents the results of the modelling activity of the West African Power Pool (WAPP). The section is divided into two parts:

— The results describing the current scenario based on 2015 data (section 4.1), which intends to validate the model through the replication of the available historical data.

— Results for a near-future scenario (section 4.1.3), which serves to test the behaviour of the model under new assumptions.

The WAPP was established in 2001 and consists of 14 member states. It is an institution of ECOWAS (Economic Community Of West African States) and its objective is to integrate the national electricity networks in a unified regional market. The countries parts of the WAPP are listed in Table 12.

Figure 8. WAPP countries[36]

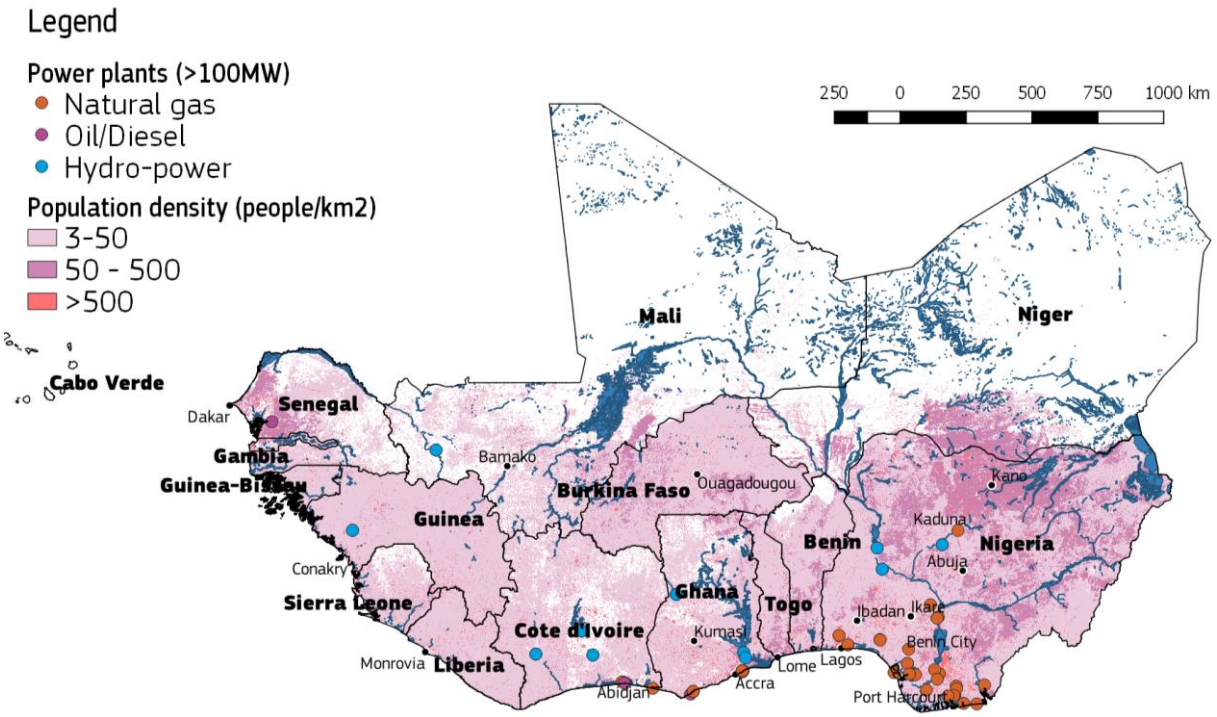

[36] Only the cities with more than 1 million of population are shown.

Table 12. Statistics for the WAPP member states from the World Bank Data[37].

Country name and ISO-3 code	Population 2017 (change from 2010), millions	GDP per capita 2017 (change from 2010), USD	Electricity consumption per capita 2015 (change from 2010), kWh	Electricity use rate (total, urban and rural (2012), %
Nigeria (NGA)	190.9 (+32.3)	1969 (-359)	144 (+8)	16/62/14.7
Ghana (GHA)	28.8 (+4.3)	1641 (+329)	355 (+74)	52/70/32
Cote d'Ivoire (CIV)	24.3 (+3.9)	1662 (+443)	276 (+60)	25/45/3
Niger (NER)	21.4 (+5.1)	378 (+30)	51 (+7)	9/45/1
Burkina Faso (BFO)	19.2 (+3.6)	671 (+95)	-	17/56/2
Mali (MLI)	18.5 (+3.5)	825 (+116)	-	23/34/7
Senegal (SEN)	15.9 (+2.9)	1033 (+31)	223 (+24)	42/70/21
Guinea (GIN)	12.7 (+1.9)	825 (+178)	-	18/69/2
Benin (BEN)	11.2 (+2.0)	830 (+72)	100 (+5)	27/55/8
Togo (TGO)	7.8 (+1.3)	617 (+129)	153 (+30)	30/53/11
Sierra Leone (SLE)	7.6 (+1.1)	499 (+100)	-	13/4/16
Liberia (LBR)	4.7 (+0.8)	456 (+129)	-	6/10/2
Gambia (GMB)	2.1 (+0.4)	483 (-79)	-	31/39/18
Guinea-Bissau (GNB)	1.9 (+0.3)	724 (+177)	-	5/10/0.4

The differences between the two scenarios simulated and analysed in this section are summarised in Table 13.

[37] The statistics are retrieved from the World Bank Data Catalog and are based on the following indicators: SP.POP.TOTL, NY.GDP.PCAP.CD, SI.POV.DDAY and EG.USE.ELEC.KH.PC. All the indicators can be downloaded and visualised from the following URL: https://data.worldbank.org/indicator/

Table 13: Summary of the characteristics of the two scenarios

Assumption	Current scenario	Future scenario
Hydrological input	LISFLOOD model outputs for the period 1979-2010	
Power plants and interconnections	Historical data as of 2015	Planned infrastructure by 2022
National electricity demand	Estimation (see section 3.3) based on 2015 data	"Current" scenario multiplied by a coefficient to match the projections for year 2022

4.1 Current scenario

This scenario is based on the WAPP situation in 2015, and is intended to test up to what extent the model is able to replicate the historical statistics. The input data for the models is based on the data described in Section 3. A visual summary of the scenario is shown in Figure 9, where we illustrate for each country the power generation mix and the transmission infrastructures as of 2015. The pie charts show the types of electricity source available in the national power systems. The red lines represent the transmission lines and areas in light red are the countries without any cross-border transmission infrastructure. It is worth noting that:

- Overall, the WAPP system is purely hydrothermal, with negligible wind and solar capacity installed. In some cases (Benin, Gambia, Guinea-Bissau, Niger, and Senegal) there is no hydro capacity despite having water resources.
- The transmission lines do not connect all the WAPP countries: Guinea, Guinea-Bissau, Gambia, Liberia and Sierra Leone do not have any cross-border transmission infrastructure. New transmission lines for those countries are currently under development as part of the CLSG (Interconnection Côte d'Ivoire-Liberia-Sierra Leone-Guinea), OMVG (The Gambia River Basin Development Organisation) and Hub Intrazonal projects.

The future scenario, later presented in Section 4.1.3, includes all the committed and planned cross-border transmission projects expected to be operational by 2022.

Figure 9. Summary of the current scenario for WAPP.

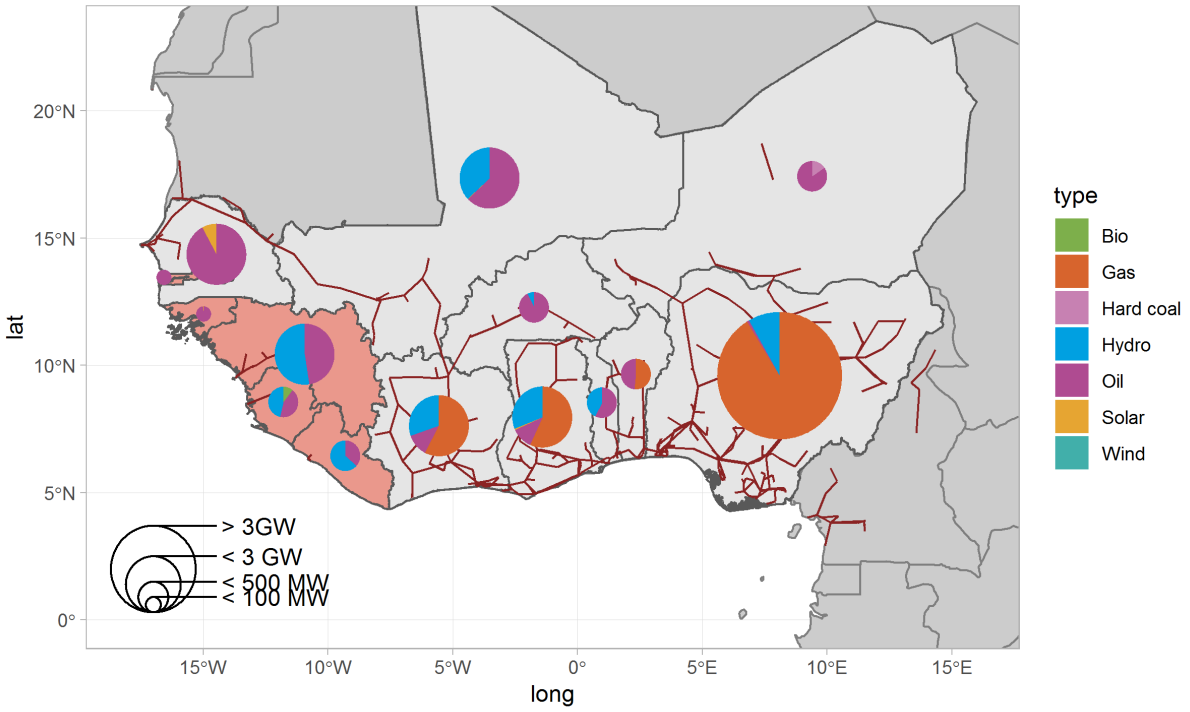

To simulate this scenario we have used the models for the MTHC and the UCD (see Section 2.1 and 2.2). The first model is used to generate the storage level for all the hydro-power reservoirs and, differently from the second, it is based on a clustered version of the input data. Thus, instead of considering all the single power-plants in the linear optimization problem, they have been clustered by fuel type and country. Thus, we have a "virtual" power plant for each combination of fuel type and country with a label formed by the country code and the Dispa-SET fuel code (see Table 3). For example instead of simulating all the natural gas (GAS) power plants in Nigeria (NGA) we consider a single virtual gas power-plant for that country, labelled 'NGA_GAS', with the capacity equal to the sum of all the power-plants. Table 15 summarises the installed capacity for each country and, except for the hydro-power, each table cell represents a single "virtual" power plant.

The clustering strategy described in the previous paragraph is applied differently for hydro-power plants, in order to be able to simulate in detail their operations and the reservoirs' dynamics. For the hydro-power generation, for each country we group all the power plants with an installed capacity below 50 MW. The virtual power plant created by this clustering approach has for capacity and storage volume the sum of the capacity and storage volumes of the single power plants, and for the nominal head is instead weighted average based on the reservoir volume. The clustered plants are labelled with a name created combining the country code and the technology of the hydro-power plants (HDAM for reservoir-based and HROR for run-of-river).

Then, in total we take into account for this scenario 14 single hydro-power plants and 13 virtual power plants (aggregation of real facilities), as summarised in Table 14. A visual summary of the hydro-power plants is shown in Figure 10.

Table 14. List of the hydro-power plants simulated in the WAPP current scenario.

Plant name	Country	Clustered	Capacity (MW)	Reservoir volume (hm^3)	Nominal head (m)
Akosombo	**GHA**	No	540	147 960	69
Shiroro	**NGA**	No	365	6 050	105
Jebba	**NGA**	No	361.8	1 000	40
Kainji	**NGA**	No	328.9	12 000	66
Bui	**GHA**	No	293.3	12 570	110
Kaleta	**GIN**	No	225.6	23	23
Taabo	**CIV**	No	165.4	69	34
NGA_HDAM	**NGA**	Yes (19)	164.5	4 916.3	40
Kossou	**CIV**	No	153.1	27 675	58
Manantali[38]	**MLI**	No	150.4	11 270	70
Buyo	**CIV**	No	145.6	8 300	37
Mount Coffee	**LBR**	No	82.7	238.6	19
Kpong	**GHA**	No	75.6	-	-
Garafiri	**GIN**	No	66.4	1 600	80
Nangbeto	**TGO**	No	58	1 710	44
SLE_HDAM	**SLE**	Yes (2)	46.5	665	82
CIV_HDAM	**CIV**	Yes (3)	45.3	994	30
Selingue	**MLI**	No	38.5	2 170	23
MLI_HROR	**MLI**	Yes (2)	30.4	-	-
SLE_HROR	**SLE**	Yes (4)	21.9	-	-
Kpime	**TGO**	No	15	0.9	16
Firestone	**LBR**	No	4.5	-	-
GIN_HDAM	**GIN**	Yes (2)	3.5	225	31
BFA_HDAM	**BFA**	Yes (2)	17/7	3 750	46
GIN_HROR	**GIN**	Yes (3)	1.9	-	-
BFA_HROR	**BFA**	Yes (2)	1.6	-	-
Tunga	**NGA**	No	0.4	-	-

[38] The Manantali dam was planned by the OVMS (Organization for the Development of the Senegal River), a joint initiative of Mali, Senegal and Mauritania. The three countries have agreed to a fixed proportional share of the electricity generated by the plant: Mali 52%, Senegal 33% and Mauritania 15% Source: http://documents.worldbank.org/curated/en/350411468154774818/pdf/773070v60ESMAP0Manantali0Generation.pdf

Table 15. Summary of the installed capacity for WAPP countries for each fuel type (MW).

Node name	Biomass	Gas	Coal	Oil	Hydro	Solar	Wind
Benin (BEN)		100		93		0.2	
Burkina Faso (BFA)		0.3		250	19		
Cote d'Ivoire (CIV)		973		200	509		
Gambia (GMB)				96		0.1	1
Ghana (GHA		1 664		330	909	22	
Guinea (GIN)				281	310	< 0.1	
Guinea-Bissau (GNB)				21		0.34	
Liberia (LBR)				51	87		
Mali (MLI)				374	219	1	
Niger (NER)			36	199			
Nigeria (NGA)	<0.1	13 608		90	1 221	1	< 0.1
Senegal (SEN)	<0.1			511		44	
Sierra Leone (SLE)	15			64	68		
Togo (TGO)				100	73		

Figure 10. Comparison of the modelled hydro-power reservoir plants in the WAPP area. Labels are shown only for the plants with a capacity greater than 150 MW.

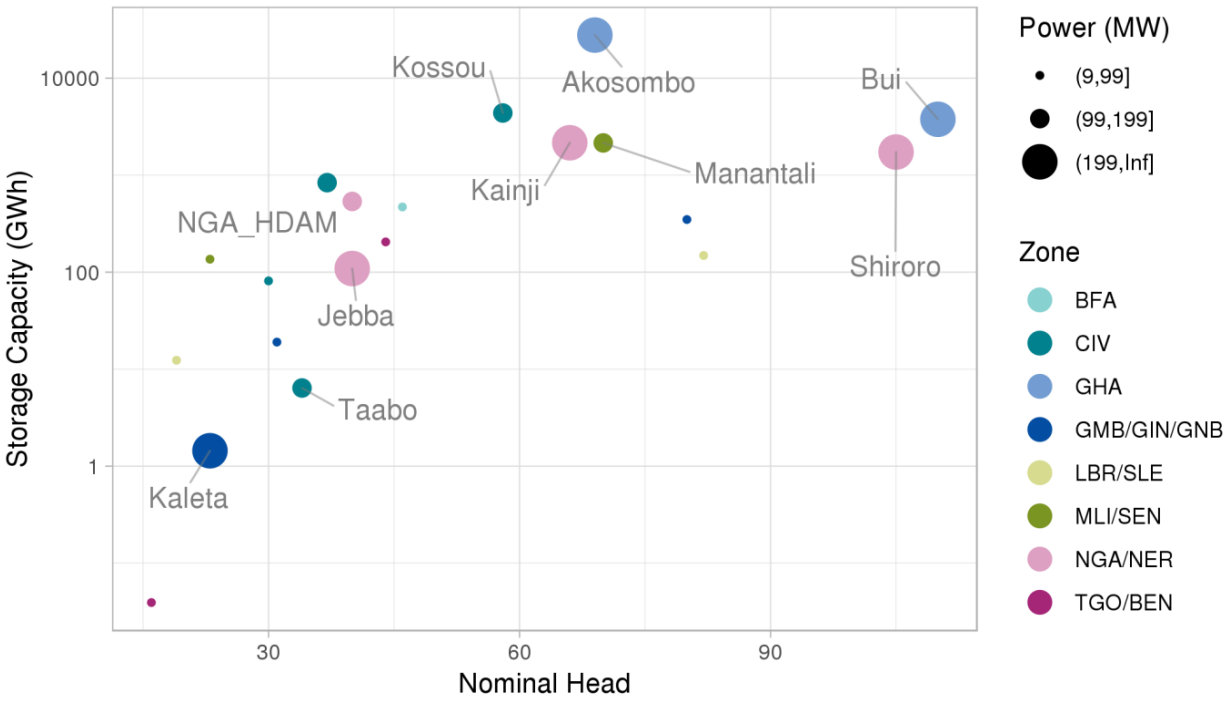

4.1.1 Definition of storage levels with Dispa-SET MTHC

The MTHC model has been used to simulate the current scenario using 32 climate years, i.e. different set of hydrological variables generated from 32 different simulations of the hydrological model. Thus, although the current scenario is based on the WAPP data for 2015, we simulate it considering 32 different inflows in order to assess the impact of the climate variability (i.e. availability of water resources) on the WAPP power system.

Each hydro-power plant shown in Table 14 has been simulated using the model described in Section 2.1 using the characteristics of each power plant (see Section 3.1.1) and an inflow generated by the hydrological model. A summary of the inflows used in the simulation is provided in the Annex 1.

The storage levels provided as output of the MTHC for the 20 modelled hydro-power reservoirs are shown in Figure 11.

Figure 11. Reservoir levels (hm^3) generated by the MTHC model for the 20 reservoir-based hydro-power plants in the WAPP. Each time-series represents a daily simulation of a different climate year. Blue line indicates the average of all climate years.

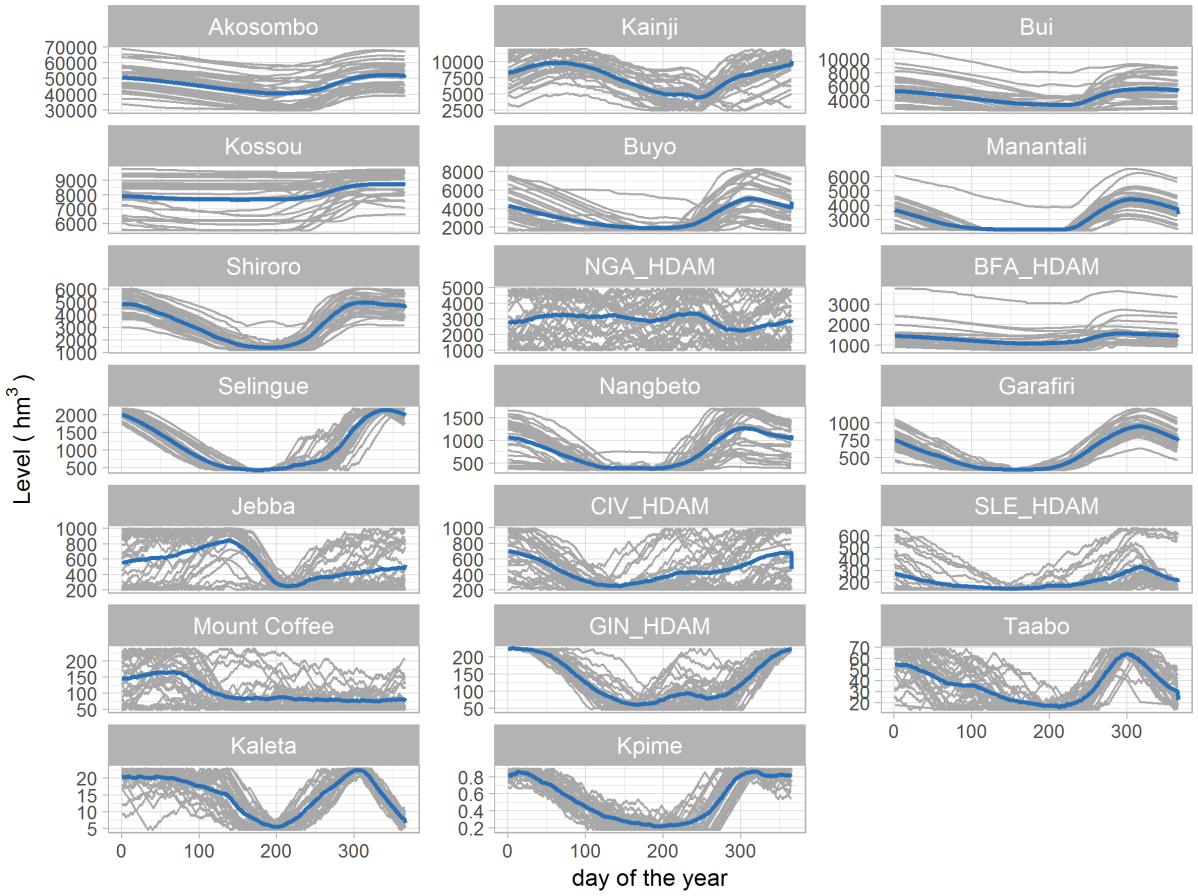

4.1.2 Hourly simulation with Dispa-SET UCD

The UCD model has been used to simulate the current scenario using the input data (as described in Section 3) and the storage levels generated by the MTHC. The simulation has also considered the 32 climate years. Differently from the MTHC, any clustering has been applied to the non-hydro generation, and then the input data include all the single non-hydro power plants. Regarding hydro-power the same list (see Table 14) has been used. The total number of power plants simulated in this scenario is 216.

In Figure 12 we can see the total energy generated in the WAPP for each fuel type (the acronyms can be found in Table 3) for each simulation with a different climate year. We can see how the most used sources of electricity are natural gas (GAS) and hydro-power (WAT). Both show an evident variability due to the meteorological factor, their inter-dependency is also shown in Figure 13, which compares the two sources for each climate year.

Figure 12. Summary of the generation by fuel type for the WAPP area.[39]

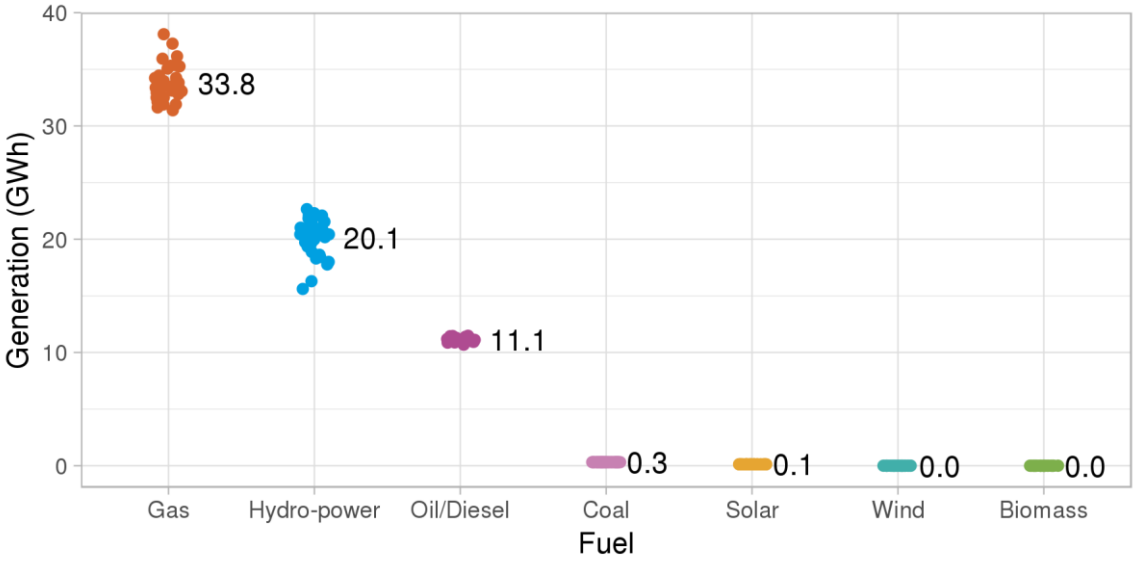

Figure 13. Comparison between yearly generation of hydro-power and gas in the WAPP area.[40]

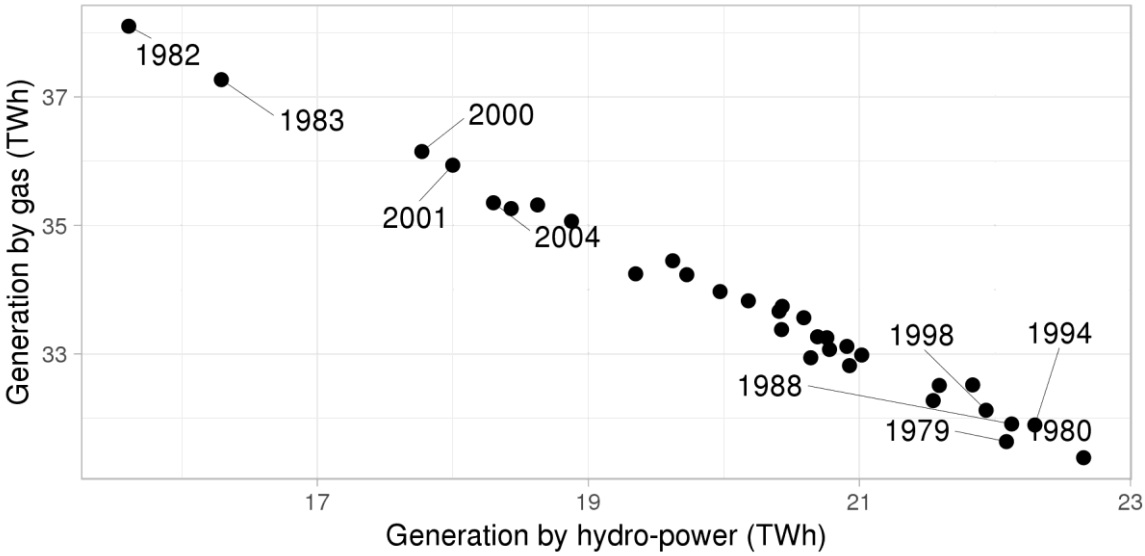

Figure 13 is useful to define the two "extremes" years, the climate year with the highest and the lowest hydro-power generation, respectively 1980 and 1982. The figure clearly illustrates how the natural gas is used to satisfy the electricity demand when there are not enough water resources available.

[39] Each point represents a simulation using a different climate year, horizontal jitter has been added to reduce overplotting. The average generation is shown as number.
[40] Each point represents a simulation using a different climate year.

A more detailed analysis on the hydro-power generation is shown in the Figure 14, where the hourly WAPP hydro-power generation is shown for all the climate years, highlighting the three wettest and the three driest years. This figure clearly illustrates the inter-annual variability due to the inflow, the seasonal pattern of daily generated electricity can vary drastically, for example during March/April and August/September.

Figure 14. Generation by hydropower for all the considered climate years. Highlighted the rolling mean for three driest and the three wettest years.

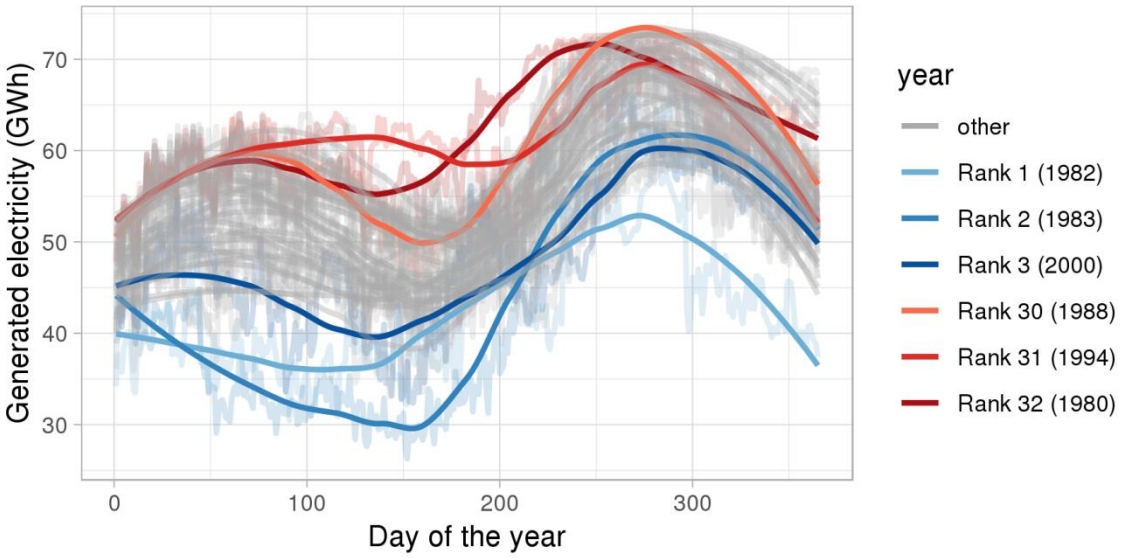

The hourly WAPP generation mix for the climate years 1980 and 1982 is shown respectively in Figure 15 and Figure 16.

Figure 15. WAPP generation mix using weather data for 1980

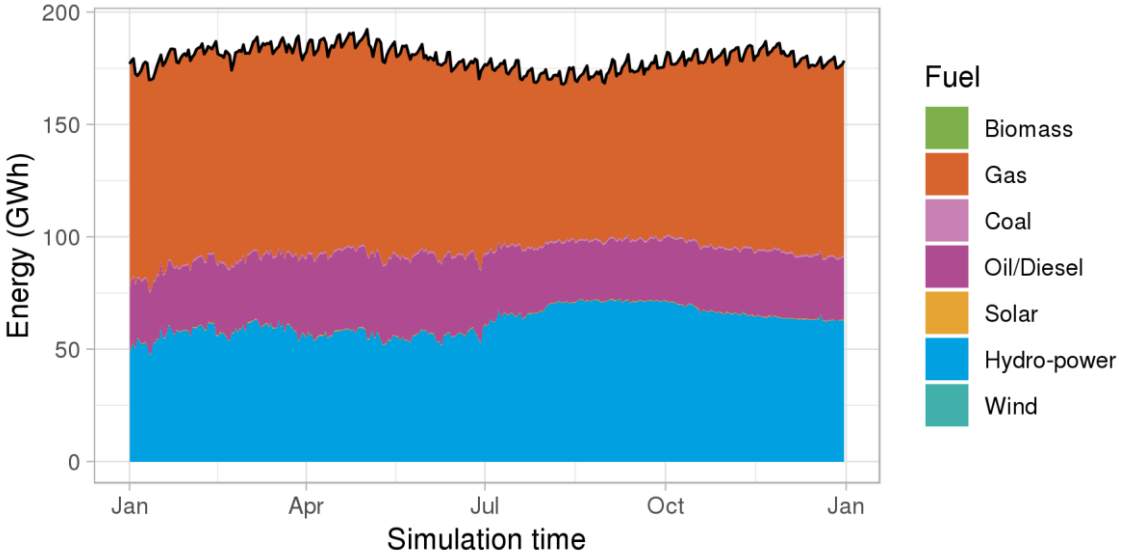

Figure 16. WAPP generation mix using weather data for 1982

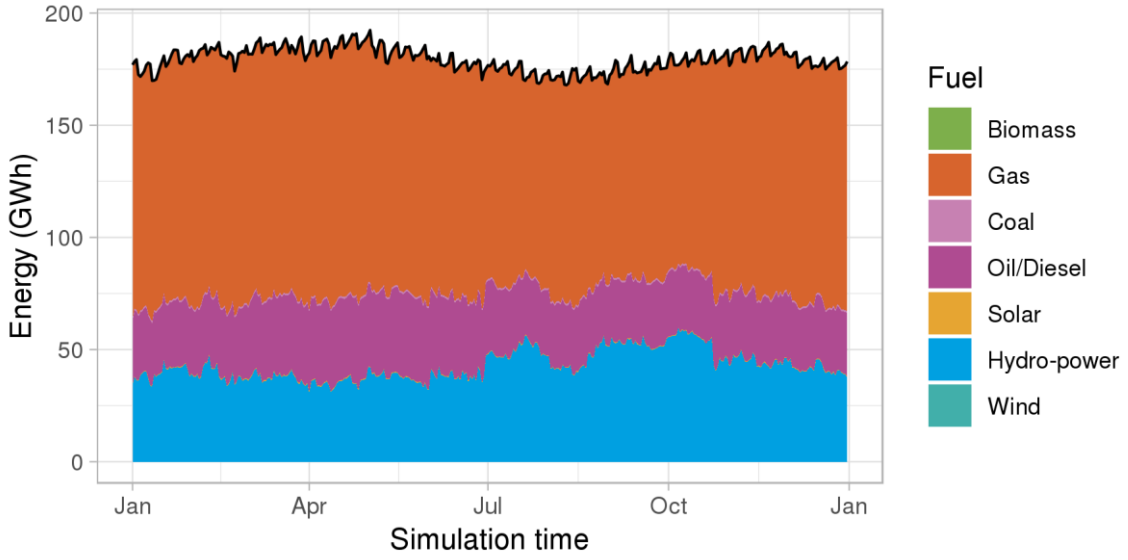

A more in-depth illustration of the electricity generation in the WAPP can be obtained looking at the regional generation, as shown Figure 17.

Figure 17. Generation mix by WAPP regions for the wettest weather year (1980, left-panel) and driest weather year (1982, right-panel)

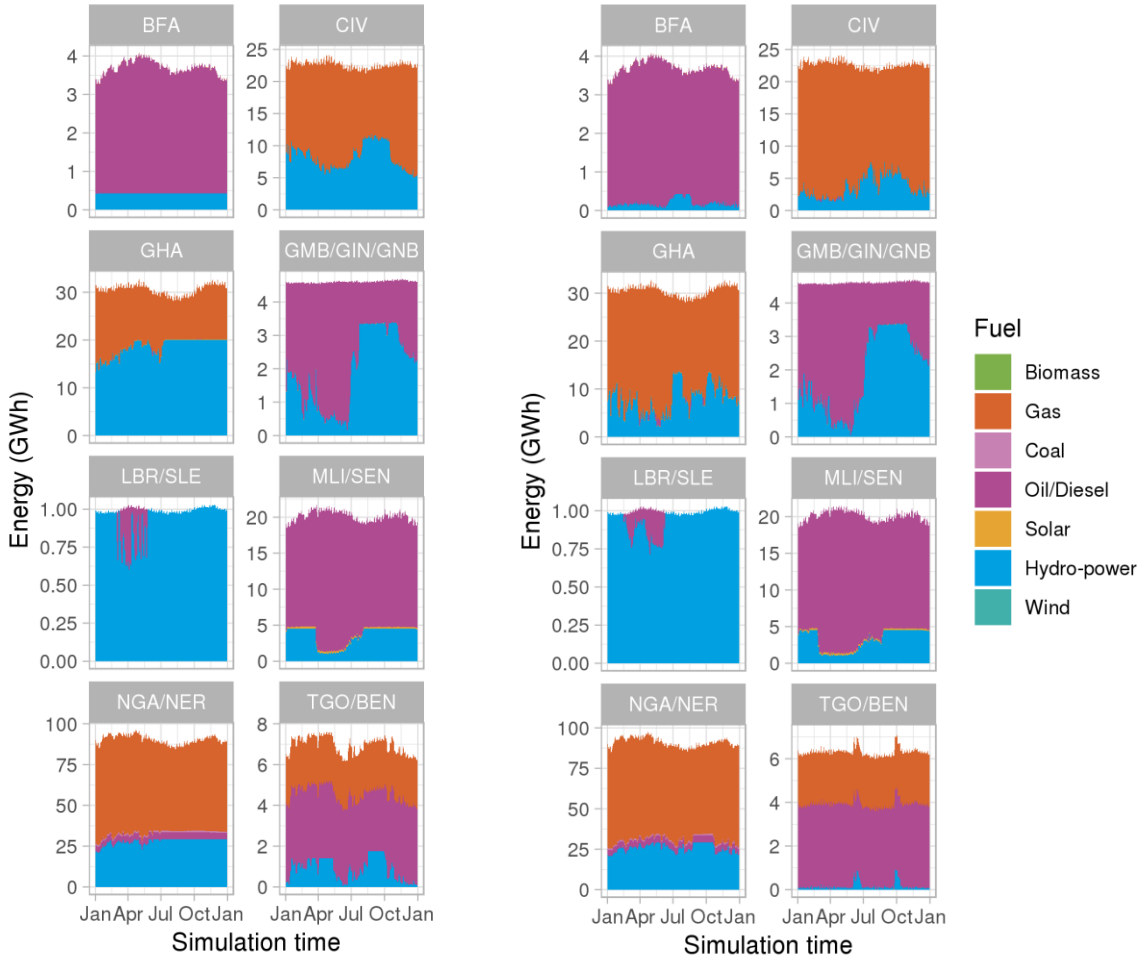

Considering the fuel prices described in section 3.2, we can define a WAPP system cost. The histogram in Figure 18 shows how the cost varies due to the climate variability. In 1980, here considered the wettest year, the system cost is 2.56 billion USD and in 1982, the driest year then with the lowest hydro-power generation, the system cost is instead 2.96 billion USD.

Figure 18. Histogram of WAPP system costs for all the climate years

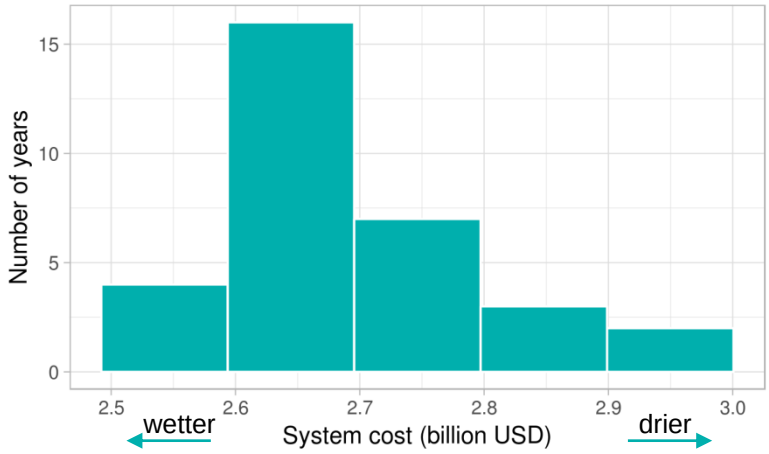

Similarly, we can estimate the emissions of carbon dioxide using the IPCC guidelines[41]. Figure 19 shows the distribution of the emissions in the current scenario for all the climate years: the CO_2 emissions are ranging from 15.6 million of tonnes in 1980 (the wettest year, thus the year with the highest availability of hydro-power) to 18.1 million of tonnes in 1982.

Figure 19. Histogram of WAPP CO_2 emissions for all the climate years

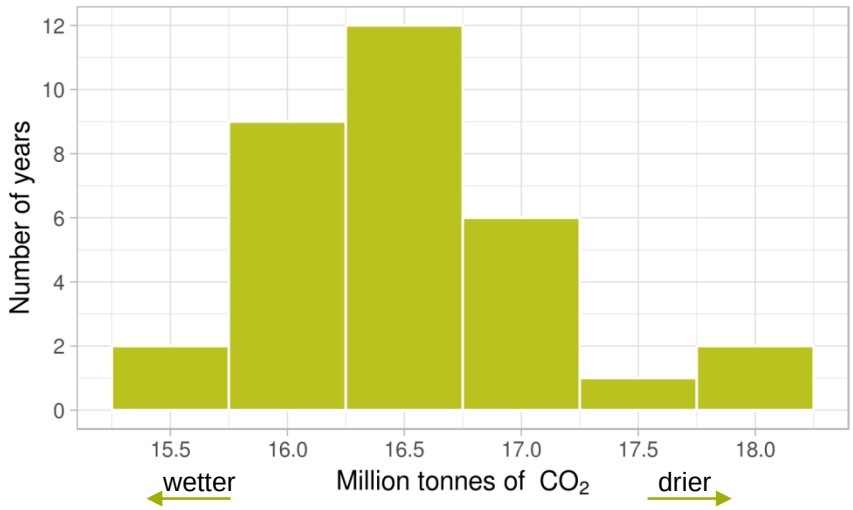

The analysis at power plant level shows (Figure 20) the units that are used to meet base load (left side cluster, mostly gas-fired power plants) and those that are used for peaking and balancing (right side cluster, mostly oil-fired), in terms of number of start-ups, as well as how the operation of the power plants change according to the availability of water resources (vertical axis).

[41] See Volume 2, Chapter 1, Table 1.4 of the 2006 IPCC Guidelines for National Greenhouse Gas Inventories (https://www.ipcc-nggip.iges.or.jp/public/2006gl/)

Figure 20. Average number of start-ups for all the thermal plants in all the climate years

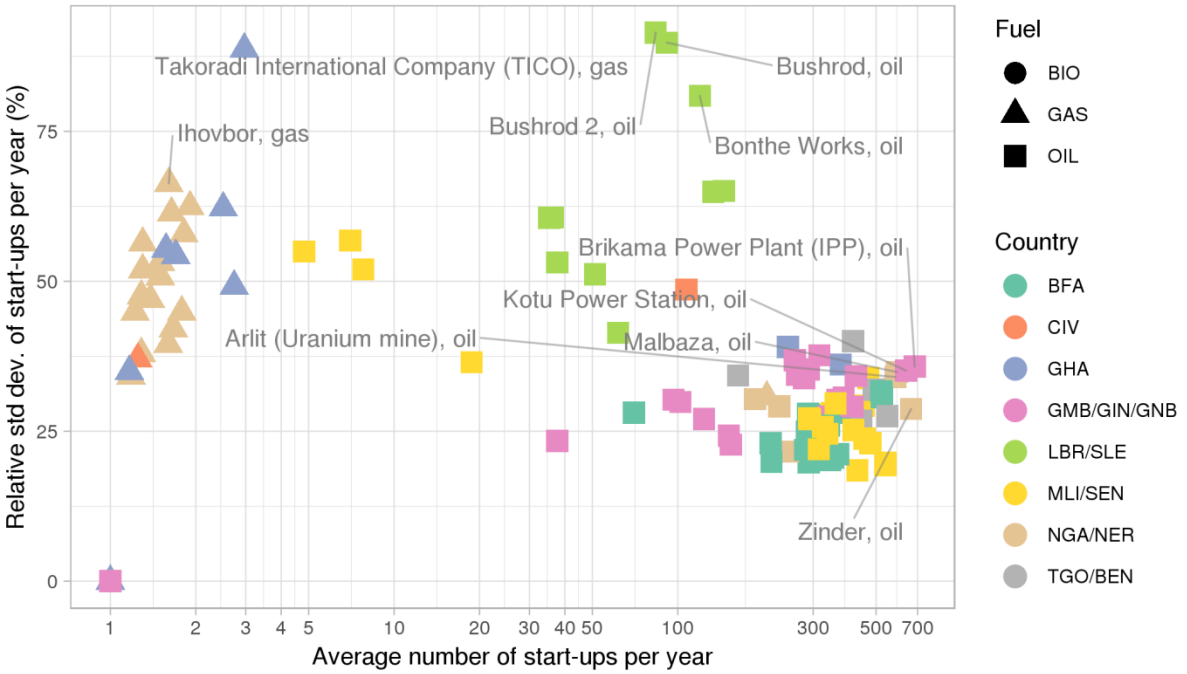

Finally, we may compare the results of the current scenario with the Africa Energy Database (AFREC) from the African Energy Commission. Figure 21 and Figure 22 show respectively the hydro-power and the thermal generation for all the WAPP countries considering all the climate years. In Figure 21 the light blue box shows the entire range obtained with all the climate years while the black line represents the average. The red dot represents the generation in 2015 from Africa Energy Database (AFREC). The simulation replicates well enough the available statistics except in the case of hydro generation in Nigeria, which is overestimated. Nigeria has the highest amount of installed capacity, with many units, but we lack more detailed information on the operational constraints (environmental limits, outages, maintenance, transmission and distribution bottlenecks, etc.) affecting them.

Figure 21. Simulated annual hydro-power generation in the WAPP countries.

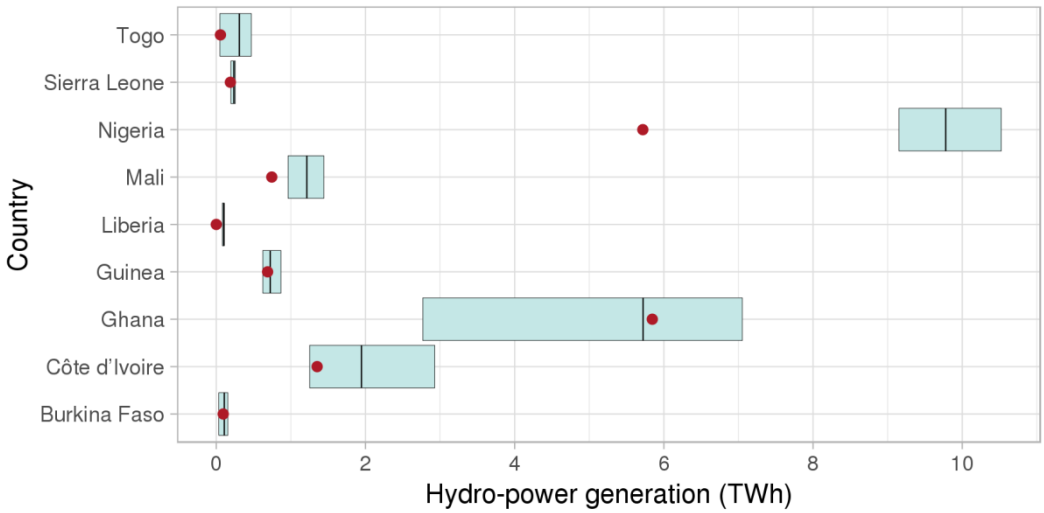

Figure 22 shows the annual generation from thermal plants. The light red box shows the entire range obtained with all the climate years while the black line represents the average. The red dot is the data from Africa Energy Database (AFREC) for 2015.

Figure 22. Simulated annual thermal power generation in the WAPP countries.

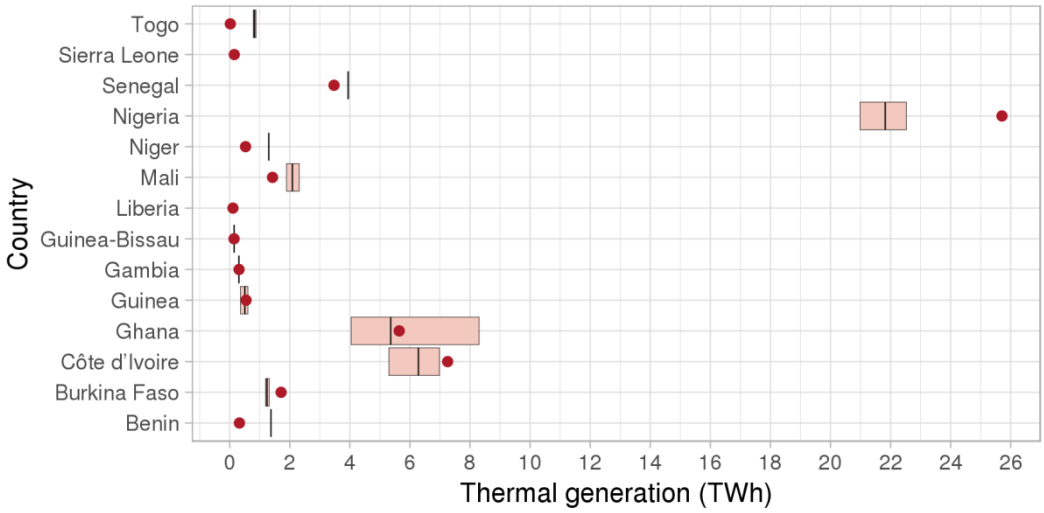

We lack information about other factors that drive the operation of the power plants, such as agreements on cross-border exchanges, long-term supply contracts, must-run conditions, or the congestion of the internal networks within each country.

4.1.3 Impact of power system operation on water availability

We have shown in Figure 11 and Figure 14 the storage levels and the hydro-power generation, respectively, for all the set the climate years.

Then, according to the methodology described in [52] and also used in [53] we may then assess the amount of water consumed in this scenario according to the climate variability. The histogram in Figure 23 shows the distribution in the consumption of water for energy generation in the WAPP from thermal power plants. In this case we have the highest consumption in the driest year with 44.4 hm^3 and then, in general, a lower consumption in the wettest years (the minimum is 29.4 hm^3 in 1994, the second wettest year), due to less use of thermal power.

Figure 23. Histogram of WAPP water consumption for energy generation for all the climate years

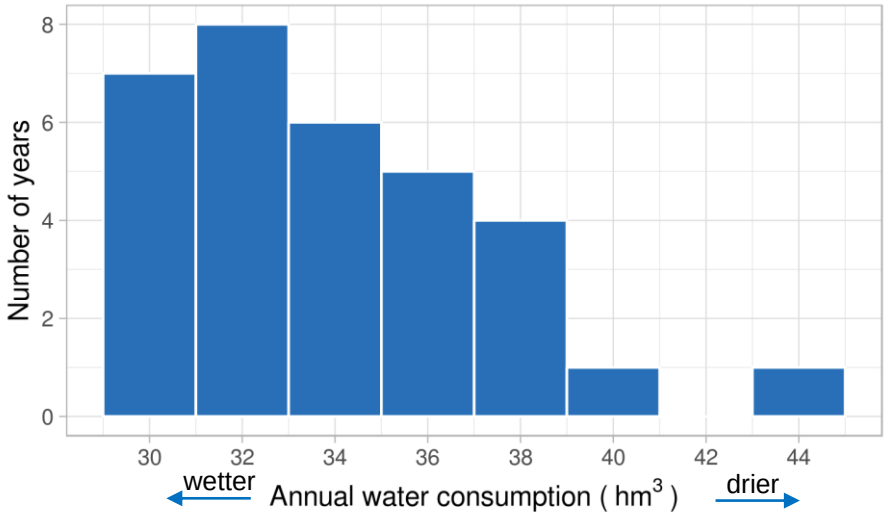

We can then disaggregate both the consumption and the withdrawal of water at monthly level as shown in Figure 24.

Figure 24. Monthly water consumption and withdrawal for all the climate years. In red the driest year (1982) and in blue the wetter (1980)

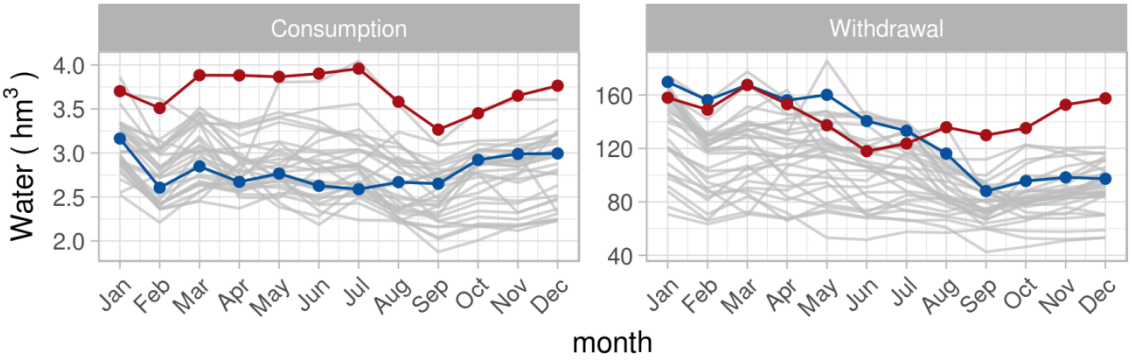

Then we can try to assess the impact of water availability on the operation of the single thermal power-plants using fresh water for cooling. For all the thermal power plants with water-based cooling, we have calculated the water withdrawal for each climate year. Figure 25 shows the water withdrawal and the generation for the ten water-cooled thermal plants with the highest generation. All the shown plants are gas-fired and, for sake of clarity, we only show the minimum, the average and the maximum of the values computed over all the weather years. In terms of water withdrawal, we can clearly see the difference between the diverse cooling methods: the tower cooling methods (used for example by Alaoji and Omotosho) in this study is considered to withdraw 4.55 cubic meters of water per MWh while the once-through technologies (used by Geregu and Egbema) withdraw 132.48 cubic meters per MWh (the values are the median values estimated in [52]). We can also observe that the majority of plants shown in the figure does not generate electricity in some years, probably due the larger availability of cheaper electricity sources (as also evidenced in Figure 13).

Figure 25. Annual water withdrawal and power generation for the 10 thermal power plants with water-based cooling with the highest average generation

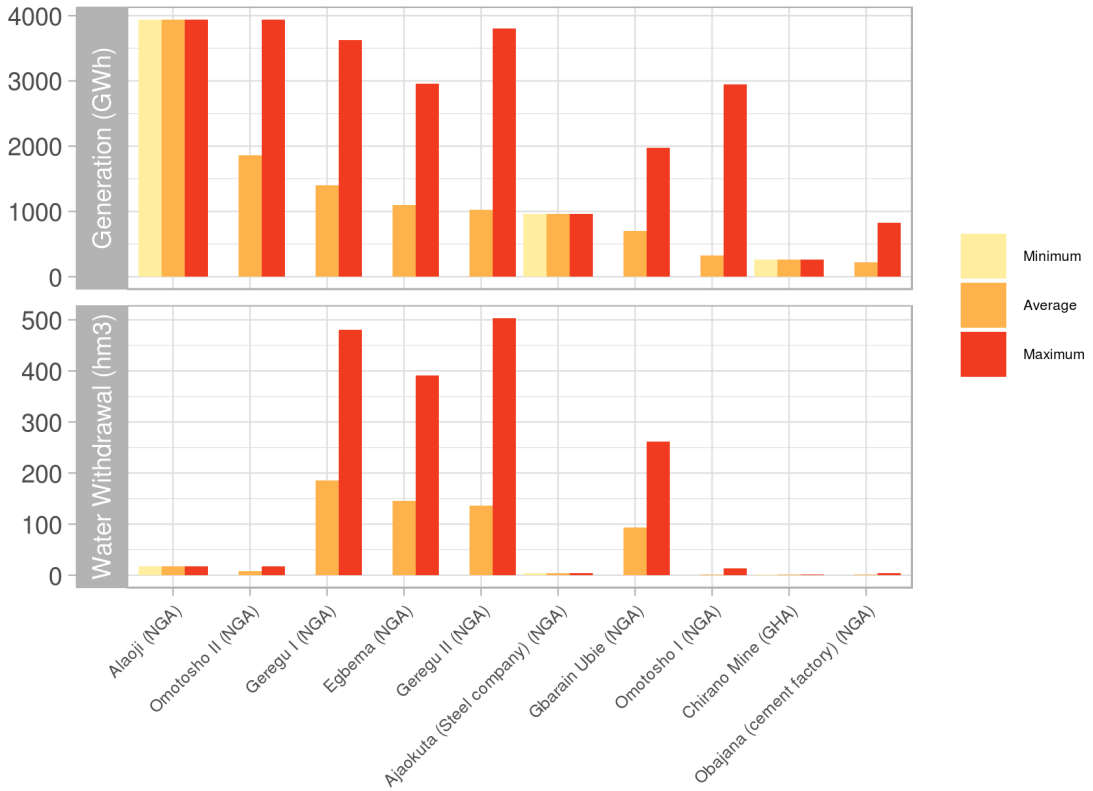

Given that the water runoff is estimated by the LISFLOOD model (the same used to provide the inflows for the hydro-power plants) for the thermal plants with a water-based cooling technology we can then define an index to quantify the water stress (the same used in [9]), i.e. the ratio between the water used for cooling and the available water (the inflow). This index can be 0 when the plant does not need water (i.e. no generation) and 1 when the plants use all the available water for cooling. In this study the index may exceed the value of 1 because the water availability has not modelled as constraint in the power system modelling. Values greater than one might indicate periods when the generation should be reduced due to the lack of available water or, also, they might be explained by the uncertainties introduced by the use of a hydrological model to simulate the inflow in a specific location or by the estimates of the water withdrawals from the study considered in this work [52].

Figure 26 presents the daily water stress index for the 450 MW gas turbine plant of Alaoji, in Nigeria. In the simulated scenario, this power plant has a similar generation in all the weather years (as also visible in Figure 25). However, the availability of water varies during the considered years thus leading to different levels of water stress. In the year with the lower inflow, we have 90 days with the water stress above 1, then indicating the impossibility to generate electricity at the maximum rate.

Figure 26: Daily water stress index calculated on all the weather years for the Alaoji gas power plant in Nigeria. The years with the highest and the lowest average index values are highlighted respectively in red and blue.

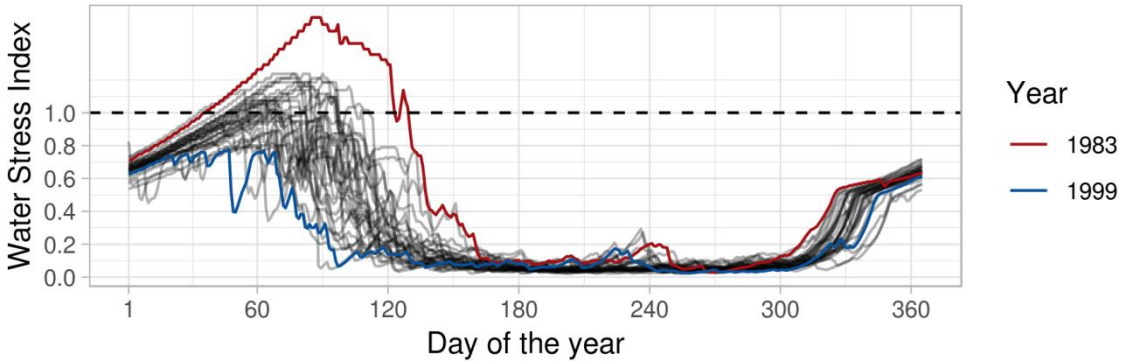

4.2 Future scenario

We define here a "future" scenario which includes the power plants and the infrastructure that are expected to be operational by 2022 according to the sources described in sections 3.1.1 and 3.1.2. The year 2022 has been chosen because in the list of the planned energy generators, the latest is expected to become operational that year.

This scenario is based on the same weather data used in the previous one. The national electricity consumptions have been obtained by considering the estimates as "Base Scenario" for year 2022 in the revised ECOWAS Master Plan[42]. The hourly values of electricity load have been estimated multiplying the values of the "current" scenario with a coefficient in order to have the annual values above mentioned. A summary of the annual demand in the two scenarios is shown in Table 16.

[42] See Tables 9-21 in the Volume 1 of "Update of the ECOWAS revised master plan for the generation and transmission of electrical energy" available at www.ecowapp.org/sites/default/files/mp_wapp_volume_1.pdf

Table 16. Summary of annual electricity demand for the current and future scenarios for the WAPP countries (TWh).

Country	Current scenario (2015)	Future scenario (2022)
Benin (BEN)	1.4	1.5
Burkina Faso (BFA)	1.3	2
Gambia (GMB)	0.3	0.9
Ghana (GHA)	11.1	19
Guinea (GIN)	1.2	2.1
Guinea-Bissau (GNB)	0.1	0.5
Ivory Coast (CIV)	8.2	11.4
Liberia (LBR)	0.1	0.4
Mali (MLI)	3.3	3.7
Niger (NER)	1.3	1.8
Nigeria (NGA)	31.4	104.6
Senegal (SEN)	4.1	5.9
Sierra Leone (SLE)	0.3	1
Togo (TGO)	1.3	1.5

Figure 27. Summary of the future scenario for WAPP (left panel) and comparison of the total amount of installed capacity with the "current" scenario (right panel).

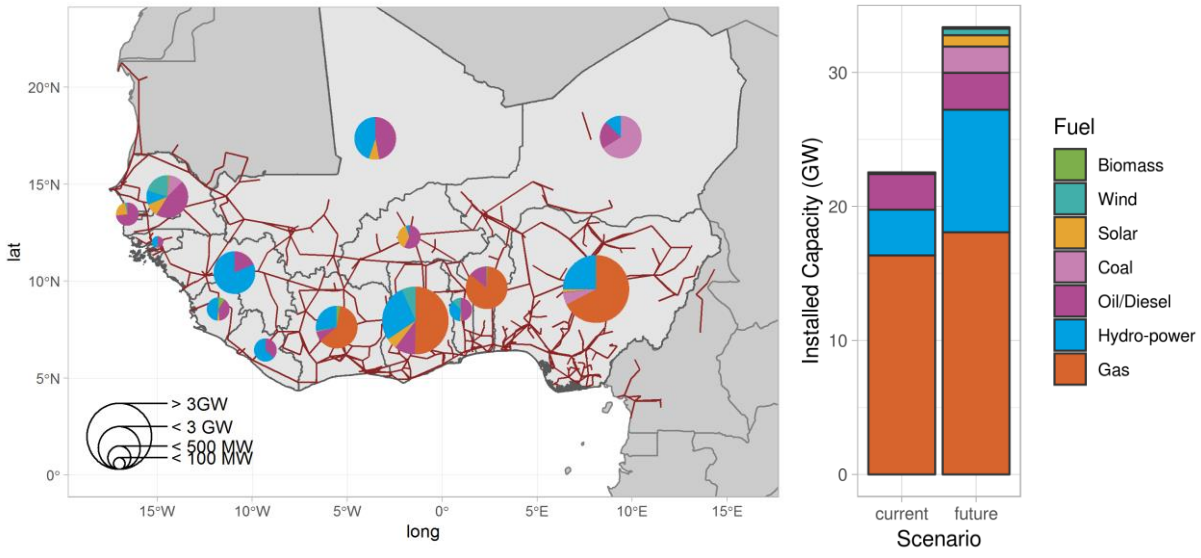

Figure 27 provides a visual summary of the future scenarios (the pie charts show the expected power generation mix and the red lines represent the transmission lines) and, compared to Figure 9, it is evident how the energy mix is more diverse. However, a detailed list of the installed capacity in this scenario is shown in Table 17. To better understand the difference between this scenario and the one presented in section 4.1, in Table 18 we can find the difference in terms of installed capacity between the two scenarios. As stated above, the new capacity is given by the new projects currently on-going or planned in the WAPP that are supposed to be operative in 2022, for example the Mambila and Zungeru dams in Nigeria, or the new coal plants of Itobe and Salkadamna in Nigeria and Niger, respectively.

Table 17. Summary of the installed capacity (MW) in the future scenario for WAPP countries for each fuel type.

Country	Biomass	Gas	Coal	Oil	Hydro	Solar	Wind
Benin (BEN)	5	550		93		0.2	
Burkina Faso (BFA)		0.3		250	21.6	164	
Cote d'Ivoire (CIV)	71	1 708		200	767.9	15	
Gambia (GMB)				96		30.1	5
Ghana (GHA		1 664		330	909	176.9	225
Guinea (GIN)				281	1 244.9	< 0.1	
Guinea-Bissau (GNB)				21	18.8	0.34	
Liberia (LBR)				51	87		
Mali (MLI)				466.1	443.1	81.8	1.1
Niger (NER)			636	199	122.2		
Nigeria (NGA)	<0.1	14 152.9	1 200	90	5 260.8	261.3	10.2
Senegal (SEN)	15		125	511	120.3	108	225
Sierra Leone (SLE)	15			64	79.7	5	
Togo (TGO)				100	73	5	25.2

Table 18. Difference in installed capacity (MW) between the future and current scenarios

Country	Biomass	Gas	Coal	Oil	Hydro	Solar	Wind
Benin (BEN)	5	450					
Burkina Faso (BFA)					2.5	164.3	
Côte d'Ivoire (CIV)	71	735			693.5	15	
Gambia (GMB)						30	4
Ghana (GHA)						155	225
Guinea (GIN)					1 143		
Guinea-Bissau (GNB)					20		
Liberia (LBR)							
Mali (MLI)				92	238	80.5	1.1
Niger (NER)			600		130		
Nigeria (NGA)		545	1 200		4 369	260	10.2
Senegal (SEN)	15		125		128	64	225
Sierra Leone (SLE)					172	5	
Togo (TGO)						5	25.2

This scenario has been simulated considering additional capacities, transmission lines and an increased demand and using the same set of climate years as used in the current scenario. However, we have limited the simulation to the two extreme years (the wettest and the driest ones, respectively 1980 and 1982) to focus only on the extremes of the distribution.

The future scenario depicts a WAPP where the energy mix is substantially different from the current one, as illustrated in Figure 28. In the figure we can see how the future power systems will rely more on natural gas (replacing oil-fired power plants) to satisfy the national electricity demand, consequently the relative share of hydro-power decreases. Furthermore, while the use of oil and diesel declines, coal – due to the additional capacities planned in Niger and Nigeria – will go from the current share almost negligible (about 0.5%) to a share of about 8%. In terms of generated electricity, the coal will contribute from the current 315 GWh to about 12 270 GWh, a 40-fold increase. The planned increase in wind and solar capacity by 2022 is expected to be minimal and therefore the share in generation will be negligible when compared with other sources.

Figure 28. Share of energy for each fuel in the two scenarios. The range is defined by the value calculated on the years 1980 and 1982, respectively the wettest and the driest among all the climate years considered. Wind, solar and biomass are excluded because negligible.

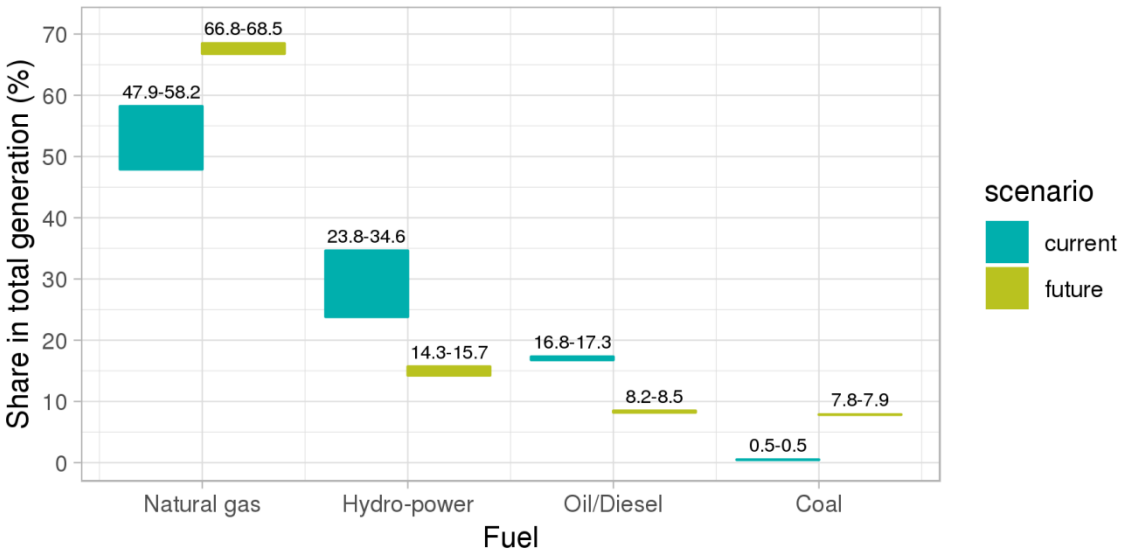

In the next figures we can see how the future scenario can be compared to the current one in terms of overall system costs, emissions and water consumption. We will show both for the current and the future scenarios only the extreme climate years, the entire distribution for the former is shown in Figure 18, Figure 19 and Figure 23.

The system cost is defined as the cost of the generated electricity considering the fuel prices described in Section 3.2. Considering that in the future scenario the electricity demand will be higher than in the current scenario (see Table 16), it is not a surprise to see (left panel in Figure 29) a substantial increase of the system cost: from 2.6-3.0 to 6.8-6.9 billions USD. Instead, if we look at the cost for generating 1 MWh of electricity in the right panel in Figure 29, we can see two important effects: firstly, the cost becomes more stable and less affected by climatic variability, and secondly, the maximum cost is lower while the minimum is higher. Both the phenomena can be explained by change in the energy generation mix: a) the reduced importance (i.e. share) of hydro-power in the future energy mix; b) the increase in the use of coal, which has a cost lower than gas and oil/diesel, and then c) in the substantial reduction in the use of oil/diesel, the most expensive among the fuels used in the WAPP system.

The CO_2 emissions in the future scenario, as for the system cost, show an evident increase, in this case both in the terms of absolute values (total emissions) and in the emissions per generated MWh of electricity. This also can be explained with the reduction in the use of hydro-power, a CO_2 emission-free source of electricity, and the increase of fossil fuels like natural gas and coal. Figure 31 describes instead the water consumed for electricity generation in the WAPP. In the left panel we can see the total consumption in millions of cubic meters. In general, we can see how in the future scenario the energy system will use more water: the left panel shows how for the driest year in the future scenario (where the electricity demand is higher than in the current scenario) the consumption of water is about three times the consumption of water in the wettest year of the current scenario.

Figure 29. Comparison of the WAPP system cost between the future and the current scenarios. In each scenario the range is estimated by considering the values for the two extreme years, 1980 and 1982, respectively the wettest and the driest. The left panel shows the total cost while the right panel shows the cost per MWh.

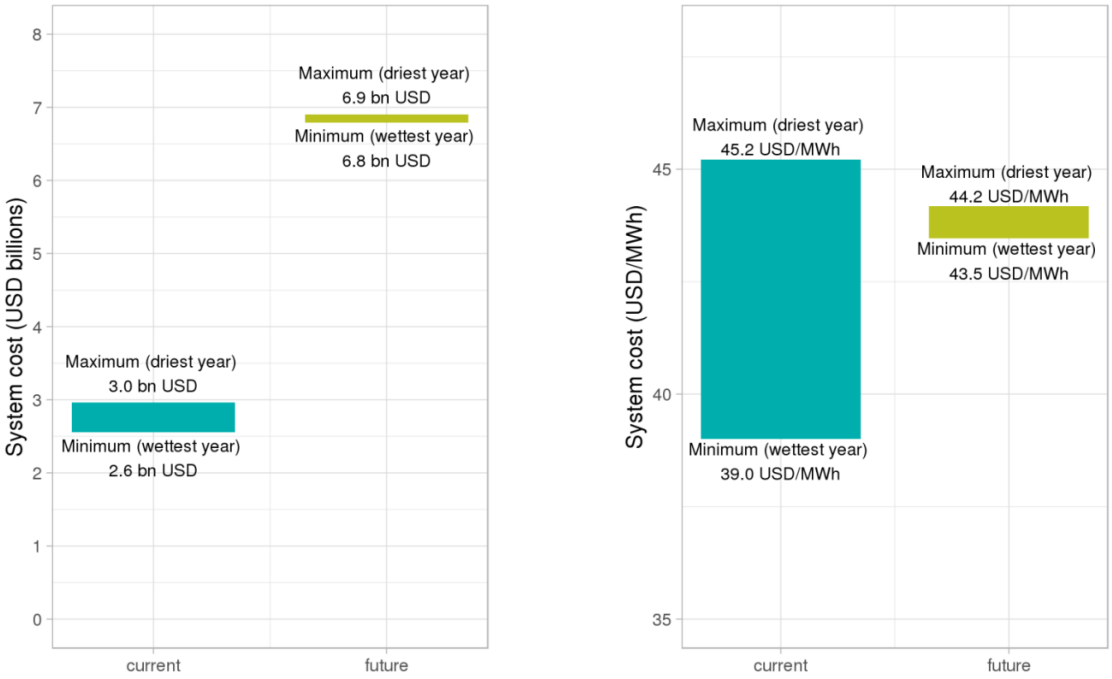

Figure 30. Comparison of the WAPP CO_2 emissions between the future and the current scenarios. In each scenario the range is estimated by considering the values for the two extreme years, 1980 and 1982, respectively the wettest and the driest. The left panel shows the total emissions while the right panel shows the emissions per MWh.

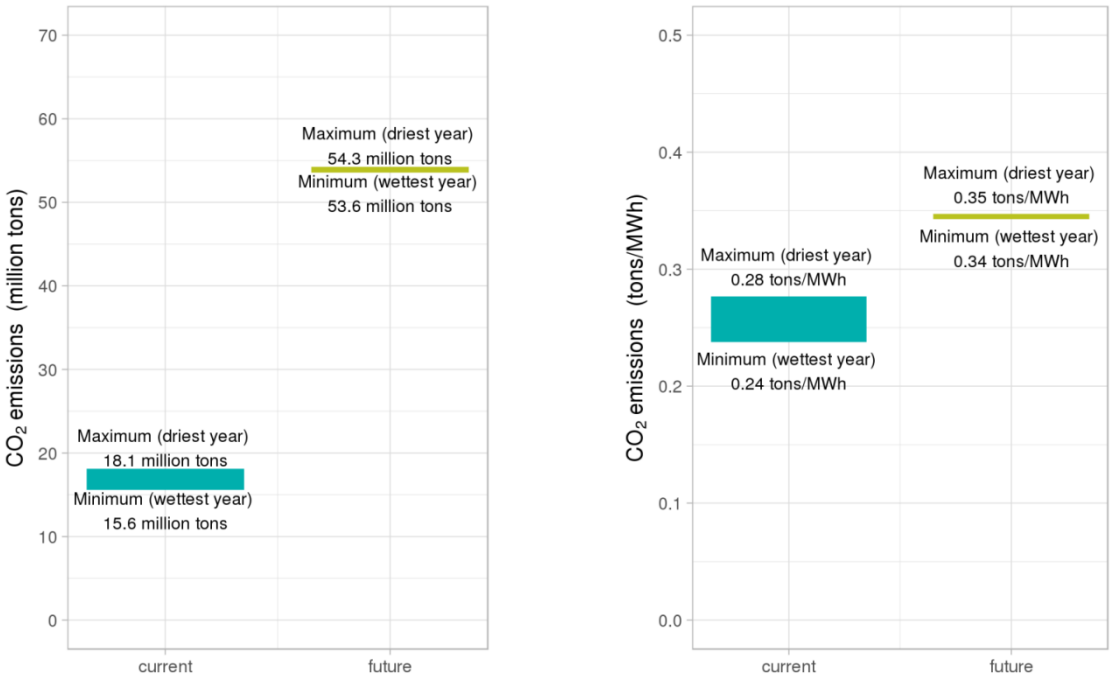

Figure 31. Comparison of the WAPP consumption of water between the future and the current scenarios. In each scenario the range is estimated by considering the values for the two extreme years, 1980 and 1982, respectively the wettest and the driest. The left panel shows the total consumption while the right panel shows the water consumption per TWh.

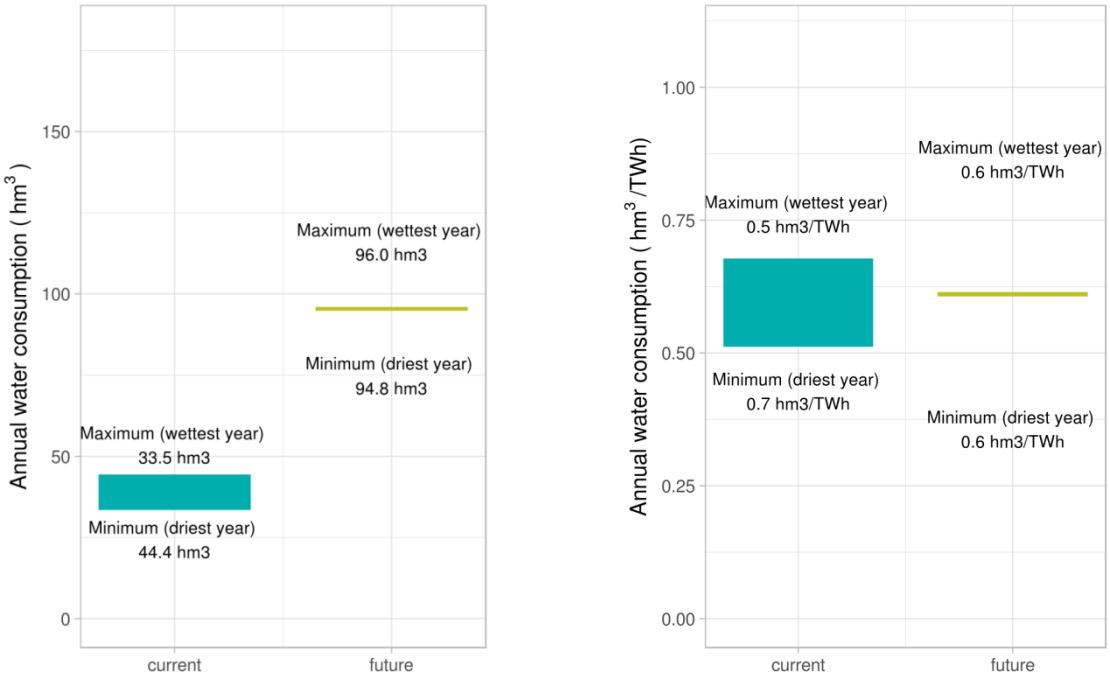

5 Conclusions

The modelling framework presented in this study provides a tool able to simulate with a very high level of detail the water-power nexus in the Western Africa Power Pool.

This level of detail and complexity is needed to carry out an in-depth analysis of the impacts of the availability of water resources on the operation of the WAPP power system.

The model can quantify the economic impacts, the emissions, the water withdrawn and consumed, and the detailed operation of the power system (scheduling and use of interconnectors) under current and future assumptions on climate conditions, energy demand, etc.

The study rests on an extensive review of data and information sources, and also provides a method to deal with the lack of detailed information on the electricity demand and the generation from renewable energy sources. The analyses of future policy cases of the WAPP will be able to build on these data, which will be made publically available.

One of the main objectives of this study has been to explore the validity of our modelling framework. We find that the Dispa-SET model behaves soundly, despite the data-related limitations, replicating the available statistics up to a great extent, and the outcomes of the simulation are robust since they are based on long time-series of climate data. Therefore the data and the model presented in this study can be used to support the design and the monitoring of energy- and water-related policies.

Even though the focus of this analysis has been on testing the validity our analysis also reveals some planning / policy related conclusions. We show that the future operation of the WAPP power system significantly depends on the availability of water resources, which is however outside the control of policy planning. This dependence translates into a high volatility of the system cost. We show that the thermal capacities scheduled to be commissioned in the WAPP master plan can mitigate this volatility to a certain extent. This however goes along with an in average higher electricity bill and increased emissions. Future policy scenarios should therefore explore which technology portfolios would be most suitable to achieve low volatility, low cost and low emissions simultaneously.

Moreover, on the technical side there are several possible improvements that could be added to the modelling framework described in this report in order to obtain more accurate results and better insights:

- Better data on the demand of electricity and water.
- Better data on the operational conditions and constraints of the power plants, thermal and hydro, the cross-border exchanges, and the national networks.
- More information about the river network and the reservoirs in order to implement cascading constraints.
- Analysis of future climate scenarios wherein the consequences of water scarcity would be exacerbated and the vulnerability of thermal power plants would be higher.
- Implement constraints on the water stress and the temperature of the water in order to better analyse extreme conditions and the vulnerability of key individual power plants (usually the ones with the highest capacity).
- Stochastic modelling to produce a more robust mid-term hydrothermal scheduling for the unit commitment model.
- Better representation of the demand of water for non-energy purposes.

In addition to the enhancements listed above, the extension of the analysis to other African power pools would allow studying the options for large-scale integration of renewable energy sources, by testing future scenarios assuming more interconnection

capacities within and between the African power pools, and analysing in more depth (e.g. impacts on water temperatures) the consequences of the interactions between the water and power system in wider areas.

References

[1] A. Hoffman, "The Water-Energy Conundrum : Can We Satisfy the Need for Both ?," *J. Energy Secur.*, no. September, 2010.

[2] I. International Energy Agency, "World Energy Outlook 2016," Paris, 2016.

[3] B. Gjorgiev and G. Sansavini, "Electrical power generation under policy constrained water-energy nexus," *Appl. Energy*, 2017.

[4] V. Nanduri and W. Otieno, "A new water and carbon conscious electricity market model for the electricity-water-climate change nexus," *Electr. J.*, pp. 64–74, 2011.

[5] S. J. Pereira-Cardenal, P. Bauer-Gottwein, K. Arnbjerg-Nielsen, and H. Madsen, "A framework for joint management of regional water-energy systems," PhD Thesis, Technical University of Denmark, 2013.

[6] S. Vassolo and P. Döll, "Global-scale gridded estimates of thermoelectric power and manufacturing water use," *Water Resour. Res.*, vol. 41, no. 4, pp. 1–11, 2005.

[7] M. T. H. Van Vliet, J. R. Yearsley, F. Ludwig, S. Vögele, D. P. Lettenmaier, and P. Kabat, "Vulnerability of US and European electricity supply to climate change," *Nat. Clim. Chang.*, vol. 2, no. 9, pp. 676–681, 2012.

[8] B. E. Jiménez Cisneros *et al.*, "Freshwater Resources," in *Climate Change 2014: Impacts, Adaptation, and Vulnerability. Part A: Global and Sectoral Aspects. Contribution of Working Group II to the Fifth Assessment Report of the Intergovernmental Panel on Climate Change*, T. E. B. Field, C.B., V.R. Barros, D.J. Dokken, K.J. Mach, M.D. Mastrandrea, S. M. M. Chatterjee, K.L. Ebi, Y.O. Estrada, R.C. Genova, B. Girma, E.S. Kissel, A.N. Levy, and and L. L. W. (eds) P.R. Mastrandrea, Eds. Cambridge, United Kingdom: Cambridge University Press, 2014, pp. 229–269.

[9] R. Fernández-Blanco, K. Kavvadias, and I. Hidalgo González, "Quantifying the water-power linkage on hydrothermal power systems: A Greek case study," *Appl. Energy*, 2017.

[10] R. Fernandez Blanco Carramolino, K. Kavvadias, and I. Hidalgo Gonzalez, "Water-related modelling in electric power systems: WATERFLEX Exploratory Research Project: version 1." Joint Research Centre, 2017.

[11] I. Hidalgo González, Q. Sylvain, and A. Zucker, "Dispa-SET 2.0: Unit commitment and power dispatch model." EUR 27015 EN, doi:10.2790/399921, pp. 1–26, 2014.

[12] P. Burek, J. van der Knijff, and A. de Roo, "LISFLOOD: Distributed water balance and flood simulation model: Revised user manual." EUR 26162 EN, doi: 10.2788/24719, pp. 1–142, 2013.

[13] K. Kavvadias, I. Hidalgo González, A. Zucker, and S. Quoilin, "Integrated modelling of future EU power and heat systems: The Dispa-SET v2.2 open-source model," 2018.

[14] "GAMS Development Corporation. General Algebraic Modeling System (GAMS) Release 24.2.1." Washington, DC, USA, 2013.

[15] K. Kavvadias, I. Hidalgo González, A. Zucker, and S. Quoilin, "Integrated modelling of future EU power and heat systems: The Dispa-SET v2.2 open-source model," 2018.

[16] "IBM ILOG CPLEX Optimisation Studio." .

[17] C. Ndehedehe, J. Awange, N. Agutu, M. Kuhn, and B. Heck, "Understanding changes in terrestrial water storage over West Africa between 2002 and 2014," *Adv. Water Resour.*, vol. 88, pp. 211–230, 2016.

[18] D. de Condappa, A. Chaponnière, and J. Lemoalle, "A decision-support tool for

water allocation in the Volta Basin," *Water Int.*, vol. 34, no. 1, pp. 71–87, 2009.

[19] P. Gyau-Boakye, "Environmental impacts of the Akosombo dam and effects of climate change on the lake levels," *Environ. Dev. Sustain.*, vol. 3, no. 1, pp. 17–29, 2001.

[20] E. Mortey, E. Ofosu, D. Kolodko, and A. Kabobah, "Sustainability Assessment of the Bui Hydropower System," *Environments*, vol. 4, no. 2, p. 25, 2017.

[21] F. A. Diawou and J. Kamiński, "An analysis of the Ghanaian power generation sector using an optimization model," *J. Power Technol.*, vol. 97, no. 1, pp. 15–27, 2017.

[22] O. Adegun, O. Ajayi, G. Badru, and S. Odunuga, "Water, energy and agricultural landuse trends at Shiroro hydropower station and environs," *Proc. Int. Assoc. Hydrol. Sci.*, vol. 376, pp. 35–43, 2018.

[23] D. O. Olukanni, A. Adejumo, and W. Salami, "Assessment of jebba hydropower dam operation for improved energy production and flood management," *ARPN J. Eng. Appl. Sci.*, vol. 11, no. 13, pp. 8450–8467, 2016.

[24] D. O. and A. W., "Assessment of Impact of Hydropower Dams Reservoir Outflow on the Downstream River Flood Regime – Nigeria's Experience," *Hydropower - Pract. Appl.*, 2012.

[25] T. S. Abdulkadir, A. W. Salami, A. R. Anwar, and A. G. Kareem, "Modelling of hydropower reservoir variables for energy generation: neural network approach," *Ethiop. J. Environ. Stud. Manag. Vol.*, vol. 6, no. 3, pp. 310–316, 2013.

[26] J. O. Aribisala, "Water Use Forecast for Hydropower Generation," vol. 2, no. 1, pp. 222–222, 2007.

[27] A. W. Salami, B. F. Sule, and O. G. Okeola, "Assessment of Climate Variability on Kainji hydropower reservoir," *Annu. Conf. Natl. Assoc. Hydrol. Sci.*, no. 2001, 2011.

[28] A. . I. D . B . Adie and M. . M. . M. and U. . B. . Aliyu, "Analysis of the Water Resources Potential and Useful Life of the Shiroro Dam , Nigeria," *Niger. J. Basic Appl. Sci.*, vol. 20, no. 4, pp. 341–348, 2012.

[29] M. A. Aminu and U. G. Kangiwa, "Performance evaluation and efficiency improvement for Jebba, Kainji and Shiroro hydro power schemes," *3rd IEEE Int. Conf. Adapt. Sci. Technol. ICAST 2011, Proc.*, no. Icast, pp. 115–118, 2011.

[30] C. R. I. M. Son, M. J. Mamman, O. Y. Matins, and J. Ibrahim, "Analysis and Characterization of Kainji Reservoir Inflow System," vol. 1, pp. 4–6, 2018.

[31] A. B. Adegbehin, Y. O. Yusuf, E. O. Iguisi, and I. Zubairu, "Reservoir inflow pattern and its effects on hydroelectric power generation at the Kainji Dam, Niger State, Nigeria," in *Proceedings of the 3 International rd Conference on Environmental and Economic Impact on Sustainable Development (EID 2016)*, 2016, vol. 203, no. Eid, pp. 233–244.

[32] E. O. E. Fergus and E. S. Ike, "Kainji Hydro Power Station Generator Availability and Unit Performance Studies," *Int. J. Eng. Innov. Res.*, vol. 3, no. 6, 2009.

[33] P. Bromand, O. Rasmussen, L. Boye, A. Issa, D. Version, and O. Rasmussen, *Screening of feasible applications of wind and solar in Mali: Assessment using the wind and solar maps for Mali*. UNEP Ris{\o} Centre on Energy, Climate and Sustainable Development. Department of Management Engineering. Technical University of Denmark (DTU), 2012.

[34] O. Ouédraogo, J. Chételat, and M. Amyot, "Bioaccumulation and trophic transfer of mercury and selenium in African sub-tropical fluvial reservoirs food webs (Burkina Faso)," *PLoS One*, vol. 10, no. 4, pp. 1–22, 2015.

[35] IRENA, "IRENA Planning and prospects for renewable power: West Africa," Abu Dhabi, 2018.

[36] C. Taliotis *et al.*, "An indicative analysis of investment opportunities in the African electricity supply sector - Using TEMBA (The Electricity Model Base for Africa)," *Energy Sustain. Dev.*, vol. 31, pp. 50–66, 2016.

[37] O. Adeoye and C. Spataru, "Sustainable development of the West African Power Pool: Increasing solar energy integration and regional electricity trade," *Energy Sustain. Dev.*, vol. 45, pp. 124–134, 2018.

[38] A. J. Conejo, J. Contreras, R. Espínola, and M. A. Plazas, "Forecasting electricity prices for a day-ahead pool-based electric energy market," *Int. J. Forecast*, vol. 21, pp. 435–462, 2005.

[39] G.-M. C. and A. J. Conejo, "Price forecasting techniques in power systems," in *Electron. Engineering*, 2001.

[40] I. González-Aparicio, J. Hidalgo, A. Baklanov, A. Padró, and O. Santa-Coloma, "An hourly PM10 diagnosis model for the Bilbao metropolitan area using a linear regression methodology," *Environ. Sci. Pollut. Res.*, vol. 20, no. 7, 2013.

[41] Pielke, *Mesoscale meteorological modelling*. 2002.

[42] M. Krutova, A. Kies, B. U. Schyska, and L. von Bremen, "The smoothing effect for renewable resources in an Afro-Eurasian power grid," *Adv. Sci. Res.*, vol. 14, pp. 253–260, Jul. 2017.

[43] T. Huld, R. Muller, and A. Gambardella, "A new solar radiation database for estimating PV performance in Europe and Africa," *Sol. energy*, vol. 86, pp. 1803–1815, 2012.

[44] I. González-Aparicio *et al.*, "Simulating European wind power generation applying statistical downscaling to reanalysis data," *Appl. Energy*, vol. 199, pp. 155–168, Aug. 2017.

[45] F. Monforti and I. Gonzalez-Aparicio, "Comparing the impact of uncertainties on technical and meteorological parameters in wind power time series modelling in the European Union," *Appl. Energy*, vol. 206, no. August, pp. 439–450, 2017.

[46] G. Olsson, *Water and Energy: Threats and Opportunities - Second Edition*. 2015.

[47] George H. Hargreaves and Zohrab A. Samani, "Reference Crop Evapotranspiration from Temperature," *Appl. Eng. Agric.*, vol. 1, no. 2, pp. 96–99, 1985.

[48] H. Tabari, "Evaluation of reference crop evapotranspiration equations in various climates," *Water Resour. Manag.*, vol. 24, no. 10, pp. 2311–2337, 2010.

[49] S. Shahidian, R. Serralheiro, J. Serrano, J. L. Teixeira, N. Haie, and F. Santos, "Hargreaves and other reduced-set methods for calculating evapotranspiration," *Evapotranspiration - Remote Sens. Model.*, vol. 23, pp. 50–80, 2012.

[50] D. P. Dee *et al.*, "The ERA-Interim reanalysis: configuration and performance of the data assimilation system," *Q. J. R. Meteorol. Soc.*, vol. 137, no. 656, pp. 553–597, Apr. 2011.

[51] Z. Huang *et al.*, "Reconstruction of global gridded monthly sectoral water withdrawals for 1971-2010 and analysis of their spatiotemporal patterns," *Hydrol. Earth Syst. Sci.*, vol. 22, no. 4, pp. 2117–2133, 2018.

[52] J. Macknick, R. Newmark, G. Heath, and K. C. Hallett, "Operational water consumption and withdrawal factors for electricity generating technologies: A review of existing literature," *Environ. Res. Lett.*, vol. 7, no. 4, 2012.

[53] H. Medarac, D. Magagna, and I. Hidalgo González, "Projected fresh water use from the European energy sector," 2018.

[54] H. Kling, P. Stanzel, and M. Fuchs, "Regional Assessment of the Hydropower Potential of Rivers in West Africa," *Energy Procedia*, vol. 97, pp. 286–293, Nov. 2016.

List of figures

List of tables

Annexes

Annex 1. Renewable energy potentials in the WAPP region

The data used for the current and near-future scenarios show that the WAPP system is purely hydrothermal. The current installed wind and solar capacity amounts to 70 MW (less than the 0.5 % of the total installed capacity) and is expected to grow up to 1340 MW (3.5% of the total capacity) by 2022. On the contrary, the hydropower capacity is 3415 MW (approximately 15% of the total installed capacity). Despite the virtually negligible amount of wind and solar capacity, the WAPP region has significant untapped potential as also pointed out by other studies, for example IRENA [35] estimates an electricity production share of wind and solar of about 10% by 2030.

For the investigation of the RES technical potential, it is important to differentiate between several categories that require different assumptions and methodological approaches. The theoretical or resource potential is the available amount of wind and solar resource that can produce energy and it depends on the estimation of wind speeds and solar irradiation reaching the area. The geographical potential is determined by the suitable and usable areas for specific RES deployment depending on an appropriate set of exclusion criteria (e.g. sloped areas, minimum distances for wind farm installations, distances to the grid, water bodies, etc.). And finally, it is necessary to define the specific technology for RES installation in each unit of available area (power density). Therefore, the estimation of the wind and solar potential by country is calculated as follows:

$$Potenial\ \left[\frac{TWh}{year}\right] = Area\ Available\ [km^2]\ x\ capacity\ factor\ x\ Power\ Density\ \left[\frac{MW}{km^2}\right] x\ 8760\ h$$

Where the areas available both for wind and solar energy, given in km^2, were extracted from the study by IRENA[43] focused on a GIS based approach.

The capacity factors were derived from the resource potential, in the section 3.4.1 and 3.4.2, the wind and solar PV generation were also calculated by KW peak per country. In the case of wind, the averaged wind speeds over each country were compared with the valued extracted from the Global Wind Atlas[44], considering the available data about wind speeds of the 10% windiest areas. The solar capacity factors were compared with the Global Solar Atlas[45] and both results had differences of less than 10 %.

The power density values considered account for standard technology used in Europe. Typical wind farms in Europe range between 5 and 8 MW/km^2, we considered 6 MW/km^2. In the case of the solar energy, assuming a range of 50-300 MW/km^2, we considered 115 MW/km^2. The assumptions defined for the power density highly influence the final technical wind and solar potential [TWh/year] and benchmarking with other sources could be misleading. Thus, before giving any estimation of the technical potential is necessary to define and set the assumptions. For example, the IRENA study on RES potentials assumed a wind power density between 18.7-20.8 MW/km^2, defined as dense arrays of wind farms such as in California. They estimated a total solar potential for Africa of 457 665 TWh / year. This output is similar (430 000 TWh/year) if we considered a power density of 20 MW/km^2. However, considering the European standard power density, the total wind potential for Africa is 63 604 TWh/year. For the case of the solar potential for Africa IRENA estimated 1 128 315 TWh/year and our estimation is similar (1 650 860 TWh/year) since the primary assumptions do not significantly differ.

Figure 32 and Figure 33 show the maps with the wind and solar technical potentials throughout the WAPP region together with shaded population density over the region. Although there are high wind and solar potential areas inland, they are found in vast desert regions in Niger, Mali, Burkina Faso, Nigeria and Liberia; where the population

[43] https://www.irena.org/-/media/Files/IRENA/Agency/Publication/2014/IRENA_Africa_Resource_Potential_Aug2014.pdf
[44] https://globalwindatlas.info/
[45] https://globalsolaratlas.info/

density is very low (about 3-5 people / km^2). That is, the areas with high wind and solar potentials are far from the consumption centres, mostly in coastal regions. Average wind and solar technical potential for the densest populated areas are up to 300 TWh and 20000 TWh for wind and solar, respectively.

Figure 34 instead represents the hydropower theoretical potential assessment provided by the ECOWREX GeoNetwork Catalog[46] at sub-catchment level. The potential is computed multiplying the mean annual discharge with the height and then with a constant representing the overall plant efficiency (87% in this study). The methodology, a discussion about its accuracy and the results is published in the report available on the ECOWREX GeoNetwork Catalog (see footnote 46) and in [54].

Figure 32. Wind technical potential (TWh/year) for the WAPP region. The grey shade represents the most populated areas.

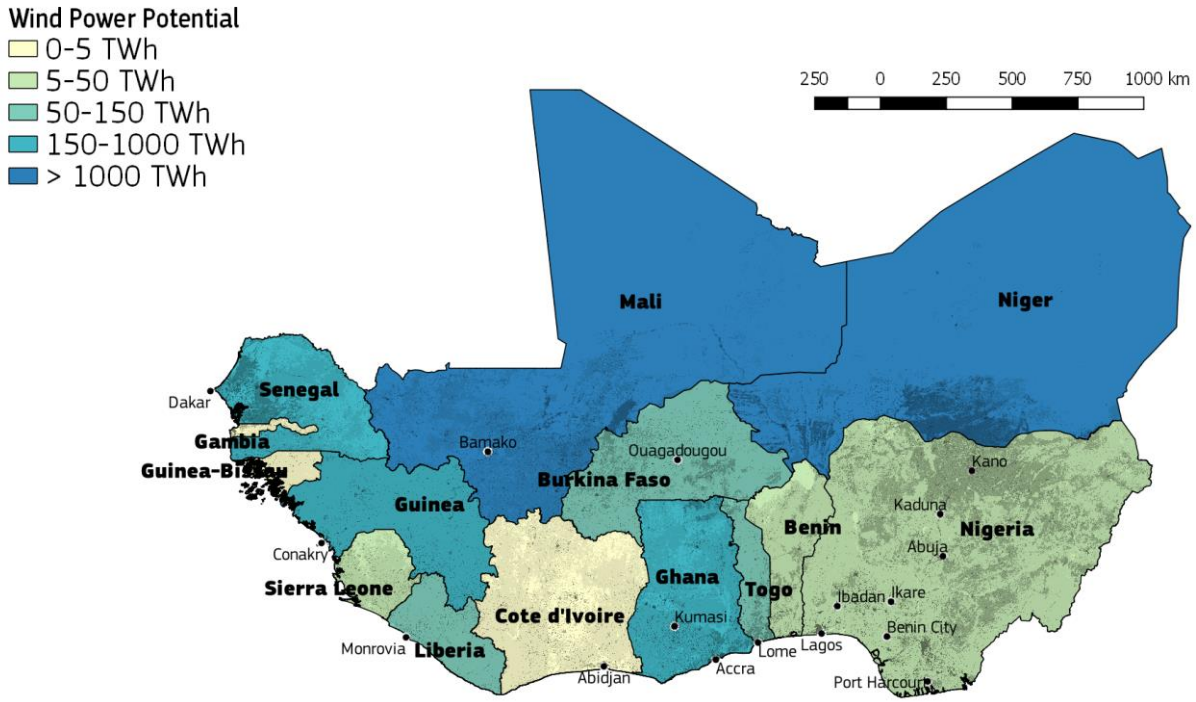

[46] The dataset is available here http://ecowrex.org:8080/geonetwork/srv/eng/catalog.search#/metadata/a46216dc-3960-4644-9650-aa8111ae6c29 under Creative Commons Attribution-Share alike 4.0 International License.

Figure 33. Solar technical potential (TWh/year) for the WAPP region. The grey shade represents the most populated areas.

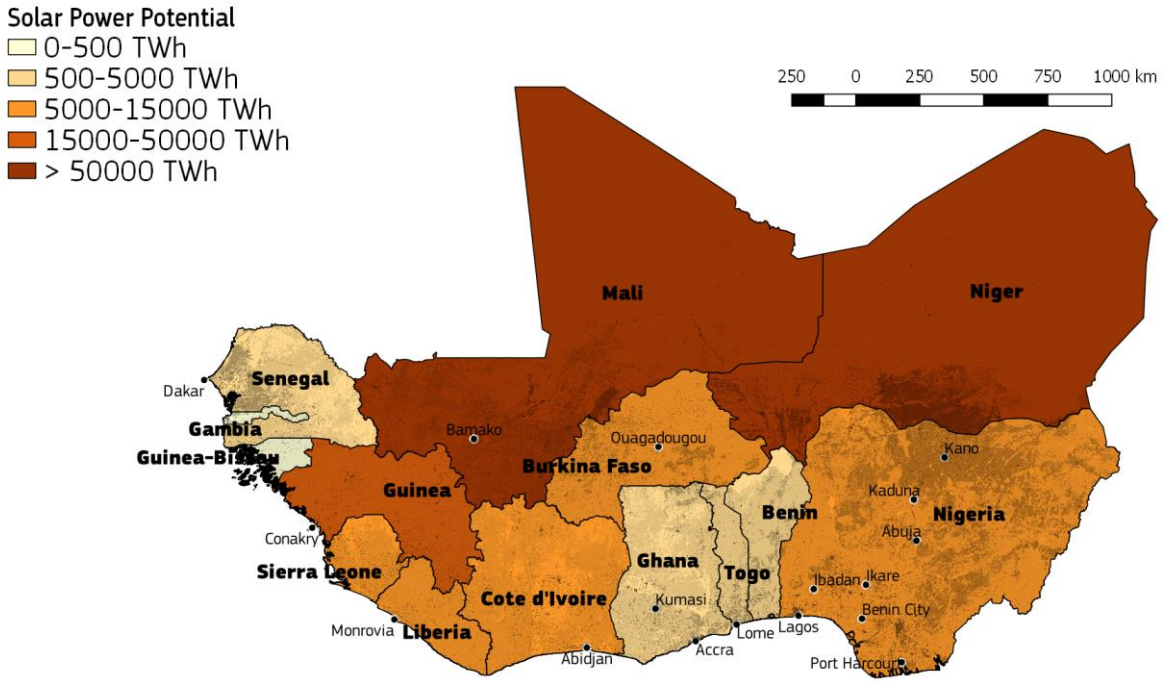

Figure 34. Hydropower theoretical potential at sub-catchment levels. Data from ECOWREX available under CC-BY-SA 4.0 license

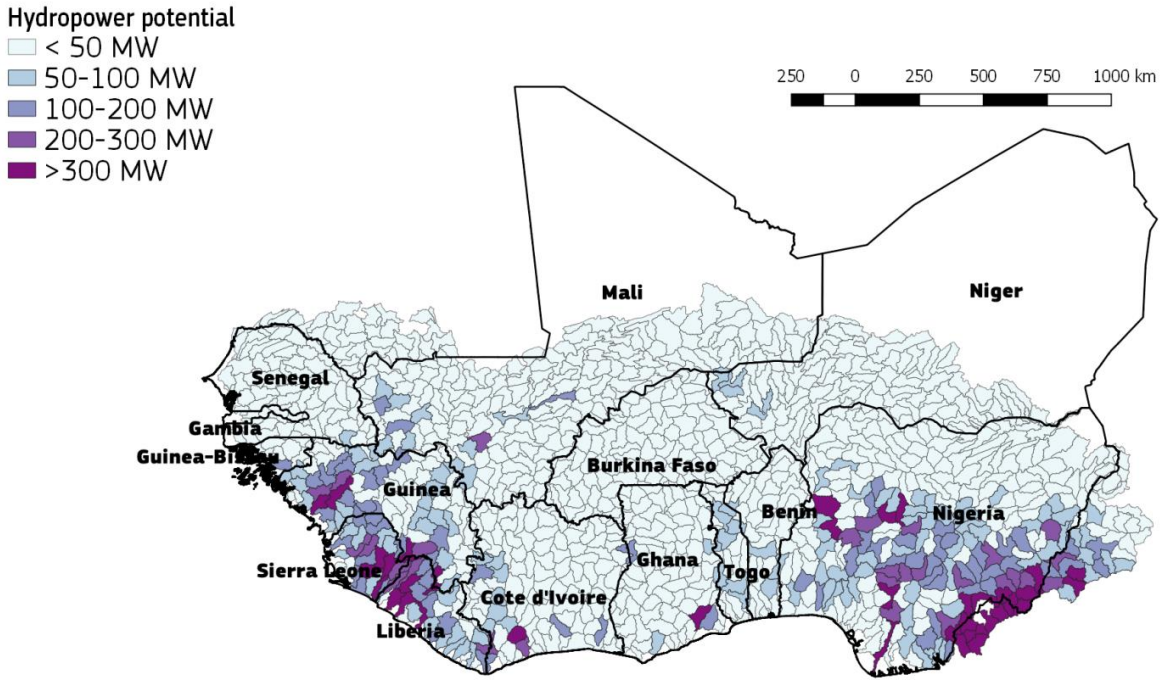

GETTING IN TOUCH WITH THE EU

In person

All over the European Union there are hundreds of Europe Direct information centres. You can find the address of the centre nearest you at: https://europa.eu/european-union/contact_en

On the phone or by email

Europe Direct is a service that answers your questions about the European Union. You can contact this service:

- by freephone: 00 800 6 7 8 9 10 11 (certain operators may charge for these calls),

- at the following standard number: +32 22999696, or

- by electronic mail via: https://europa.eu/european-union/contact_en

FINDING INFORMATION ABOUT THE EU

Online

Information about the European Union in all the official languages of the EU is available on the Europa website at: https://europa.eu/european-union/index_en

EU publications
You can download or order free and priced EU publications from EU Bookshop at: https://publications.europa.eu/en/publications. Multiple copies of free publications may be obtained by contacting Europe Direct or your local information centre (see https://europa.eu/european-union/contact_en).

KJ-NA-29617-EN-N

The European Commission's science and knowledge service

Joint Research Centre

JRC Mission

As the science and knowledge service of the European Commission, the Joint Research Centre's mission is to support EU policies with independent evidence throughout the whole policy cycle.

EU Science Hub

ec.europa.eu/jrc

@EU_ScienceHub

EU Science Hub - Joint Research Centre

Joint Research Centre

EU Science Hub

Publications Office

doi:10.2760/362802

ISBN 978-92-79-98138-8